

**ISTANBUL TECHNICAL UNIVERSITY ★ EURASIA INSTITUTE OF  
EARTH SCIENCES**

**PALEOENVIRONMENTAL INTERPRETATIONS  
FOR KIZILIRMAK DELTA PLAIN USING SEDIMENTOLOGICAL  
RECORDS, MULTIPROXY ANALYSIS AND PALYNOLOGY**

**M.Sc. THESIS**

**Gülgün ERTUNÇ**

**Department of Solid Earth Sciences**

**Geodynamics Programme**

**NOVEMBER 2016**



**ISTANBUL TECHNICAL UNIVERSITY ★ EURASIA INSTITUTE OF  
EARTH SCIENCES**

**PALEOENVIRONMENTAL INTERPRETATIONS  
FOR KIZILIRMAK DELTA PLAIN USING SEDIMENTOLOGICAL  
RECORDS, MULTIPROXY ANALYSIS AND PALYNOLOGY**

**M.Sc. THESIS**

**Glgn ERTUN  
602141001**

**Department of Solid Earth Sciences**

**Geodynamics Programme**

**Thesis Advisor: Prof. Dr. Attila İNER**

**NOVEMBER 2016**



**ISTANBUL TEKNİK ÜNİVERSİTESİ ★ AVRASYA YERBİLİMLERİ**  
**ENSTİTÜSÜ**

**KIZILIRMAK DELTASI'NDA SEDİMAN KAYITLARI, MULTİ-PARAMETRE  
YÖNTEMLER VE PALİNOLOJİ YARDIMIYLA PALEOORTAM  
YORUMLANMASI**

**YÜKSEK LİSANS TEZİ**

**Gülgün ERTUNÇ**  
**602141001**

**Katı Yerbilimleri Anabilim Dalı**

**Jeodinamik Programı**

**Tez Danışmanı: Prof. Dr. Attila ÇİNER**

**KASIM 2016**



Gülgün ERTUNÇ, a M.Sc student of ITU Graduate School of Science Engineering and Technology student ID 602141001, successfully defended the thesis entitled “PALEOENVIRONMENTAL INTERPRETATIONS FOR KIZILIRMAK DELTA PLAIN USING SEDIMENTOLOGICAL RECORDS, MULTIPROXY ANALYSIS AND PALYNOLOGY”, which she prepared after fulfilling the requirements specified in the associated legislations, before the jury whose signatures are below.

**Thesis Advisor :** **Prof. Dr. Attila ÇİNER** .....  
ISTANBUL Technical University

**Jury Members :** **Prof. Dr. Attila ÇİNER** .....  
ISTANBUL Technical University

**Assoc. Prof. Kadir ERİŞ** .....  
ISTANBUL Technical University

**Assoc. Prof. Erdal KOŞUN** .....  
AKDENİZ University

**Date of Submission : 25 November 2016**

**Date of Defense : 16 May 2017**







*To my family*



## **FOREWORD**

This thesis was carried out in the context of project Anatolian pLateau climatE and Tectonic hazards (ALerT) and funded and supported by the European Commission as part of the Marie-Curie-ITN and carried out at Solid Earth Sciences Department, Eurasia Institute of Earth Sciences, Istanbul Technical University.

I am grateful to all people that were involved in this study. In particular, I would like to thank to my advisor Prof. Dr. Attila ÇİNER for his excellent guidance and support during this process and for giving me the opportunity to take part in this ALerT project. I also wish to thank all of the colleagues from partner institutes of ALerT Project, especially Christopher BERNDT for his help in every stages of this study. I also would like to thank Dr. Marianna KOVÁČOVÁ and Müge ATALAR for introducing me palynological studies during my stay at Comenius University in Bratislava, Slovakia.

I thank to Assoc. Prof. Dr. Cengiz YILDIRIM and Assoc. Prof. Dr. M.Akif SARIKAYA for always being willing to help me during my master studies.

I am grateful to Assoc. Prof. Dr. Kadir ERİŞ for contributing his expertise in and members of ITU-EMCOL for their help and guideness during my laboratory works,

I would like to thank my friends, fellow students for their moral support.

And finally, thanks to my family for their love, encouragement, support and patience.

May 2017

Gülgün ERTUNÇ  
Geological Engineer



## TABLE OF CONTENTS

	<u>Page</u>
FOREWORD.....	ix
TABLE OF CONTENTS.....	xi
ABBREVIATIONS .....	xii
SYMBOLS .....	xv
LIST OF TABLES .....	xvii
LIST OF FIGURES .....	xix
SUMMARY .....	xxi
ÖZET.....	xxiv
1. INTRODUCTION.....	1
1.1 The Black Sea Basin History.....	2
1.2 Development of Kızılırmak Delta .....	3
1.3 Purpose of the study.....	4
1.4 Literature Review.....	5
1.5 Study Area .....	7
2. MATERIALS AND METHODOLOGY.....	8
2.1 Sediment Core and Sampling Methods.....	8
2.2 Sediment Description .....	9
2.3 Gamma Density and Magnetic Susceptibility Analysis by Multi Sensor Core Logger (MSCL).....	10
2.3.1 Gamma Density.....	12
2.3.2 Magnetic Susceptibility (MS) .....	13
2.4 Element Profiling using ITRAX XRF-Core Scanner .....	14
2.5 <sup>14</sup> C Dating of the Sedimentary Sequence.....	15
2.6 Palynology and Palynofacies Analysis.....	16
3. RESULTS .....	17
3.1 Lithostratigraphy and Chronostratigraphy .....	17
3.2 MSCL RESULTS.....	40
3.3 XRF RESULTS .....	41
3.4 AMS RESULTS.....	46
3.5 POLEN RESULTS.....	47
4. DISCUSSION .....	52
5. CONCLUSION.....	54
REFERENCES .....	55
CURRICULUM VITAE.....	58



## **ABBREVIATIONS**

<b>ALeT</b>	: Anatolian Plateau climate and Tectonic hazards
<b>AMS</b>	: Accelerator Mass Spectrometry
<b>App</b>	: Appendix
<b>BP</b>	: Before Present
<b>Bsl</b>	: Below Surface Level
<b>EIES</b>	: Eurasia Institute of Earth Sciences
<b>EMCOL</b>	: Eastern Mediterranean Centre for Oceanography and Limnology
<b>GRAPE</b>	: Gamma-Ray Attenuation Porosity Evaluator
<b>ITN</b>	: Initial Training Networks
<b>ITU</b>	: Istanbul Technical University
<b>LGM</b>	: Last Glacial Maximum
<b>MS</b>	: Magnetic Susceptibility
<b>MSCL</b>	: Multi Sensor Core Logger
<b>OSL</b>	: Optically Stimulated Luminescence
<b>PSICAT</b>	: Paleontological Stratigraphic Interval Construction
<b>VCD</b>	: Visual Core Description
<b>XRF</b>	: X-Ray Fluorescence





## **SYMBOLS**





**LIST OF TABLES**

**Page**

**Table 1. :** AMS 14C dating results

**46**





## LIST OF FIGURES

	<u>Page</u>
<b>Figure 1.</b> Map of the lowermost reach of the Kızılırmak, showing the modern delta plain and two uplifted palaeo-deltas (Akkan 1970) .....	6
<b>Figure 2.</b> The Kızılırmak Delta study area, located at 41°34'40.0"N 36°02'51.2"E. ....	7
<b>Figure 3.</b> Geotek Multi Sensor Core Logger, MSCL.....	10
<b>Figure 4.</b> Schematic diagram of a Geotek Multi Sensor Core Logger, MSCL	12
<b>Figure 5.</b> Gamma density calibration materials .....	13
<b>Figure 6.</b> ITRAX XRF core scanner .....	14
<b>Figure 7.</b> Digital photography, radiographic image and lithological description of the sediment core from 1 m bsl.....	18
<b>Figure 8.</b> Digital photography, radiographic image and lithological description of the sediment core from 1 m to 2 m bsl. ....	20
<b>Figure 9.</b> Digital photography, radiographic image and lithological description of the sediment core from 2 m to 3 m bsl. ....	22
<b>Figure 10.</b> Digital photography, radiographic image and lithological description of the sediment core from 3 m to 4 m bsl.....	24
<b>Figure 11.</b> Digital photography, radiographic image and lithological description of the sediment core from 4 m to 5 m bsl.....	26
<b>Figure 12.</b> Digital photography, radiographic image and lithological description of the sediment core from 5 m to 6 m bsl.....	28
<b>Figure 13.</b> Digital photography, radiographic image and lithological description of the sediment core from 6 m to 7 m bsl.....	30
<b>Figure 14.</b> Digital photography, radiographic image and lithological description of the sediment core from 7 m to 8 m bsl.....	31
<b>Figure 15.</b> Digital photography, radiographic image and lithological description of the sediment core from 8 m to 9 m bsl.....	33
<b>Figure 16.</b> Digital photography, radiographic image and lithological description of the sediment core from 9 m to 10 m bsl.....	35
<b>Figure 17.</b> Digital photography, radiographic image and lithological description of the sediment core from 10 m to 11 m below surface level	36
<b>Figure 18.</b> Digital photography, radiographic image and lithological description of the sediment core from 11 m to 12 m bsl.....	38
<b>Figure 19.</b> Digital photography, radiographic image and lithological description of the sediment core from 12 m to 13 m bsl.....	39
<b>Figure 20.</b> Gamma density, fractional porosity and magnetic susceptibility results .....	40
<b>Figure 21.</b> XRF/depth profiles of Si, K Ca, Ti, Cr, Mn, Fe, Ni, Zn, Rb, Sr, Zr, Pb. ....	43
<b>Figure 22.</b> Palynology results from 0-0,40 m interval .....	48
<b>Figure 23.</b> Palynology results from 1,40-1,42 m interval .....	49
<b>Figure 24.</b> Palynology results from 3,68-3,70 m interval .....	50
<b>Figure 25.</b> Palynology results from 8,50-8,52 m interval .....	51
<b>Figure 26.</b> Lithological profile and certain elemental ratios of XRF ITRAX results of the sediment core BW-1 .....	53



**PALEOENVIRONMENTAL INTERPRETATIONS FOR KIZILIRMAK  
DELTA PLAIN USING SEDIMENTOLOGICAL RECORDS, MULTIPROXY  
ANALYSIS AND PALYNOLOGY**

**SUMMARY**

The Kızılırmak Delta is the delta of the Kızılırmak River and it's located near the province of Samsun, Central Black Sea Region of northern Turkey (41°30' to 41°45' N, 35°43' to 36°08' E).

The latest major transgression of the Black Sea is related to the glacial melting accompanied with a worldwide sea level rise. The eastern Kızılırmak Delta platform is thought to be a part of a post-glacially filled canyon system, which has been incised into the former delta platform during the last glacial. The sediment fill of canyon were supplied by the Kızılırmak River. A sediment core was obtained from possible location of filled canyon system in the eastern wetlands of Kızılırmak Delta Plain. High sedimentation rate of the Kızılırmak River provide a perfect archive and continious records of the environmental and climatic conditions for Quaternary. Lithological properties, multi proxy analysis and palynological analysis were carried out from recovered sediment core and age model executed using radiocarbon analysis. By combining several techniques together, a broader data was determined and cross-correlations are made to ensure an accurate paleoenvironment reconstruction of the Kızılırmak Delta.

This thesis was carried out in the context of Anatolian pLateau climatE and Tectonic hazards (ALeRT) project, funded and supported by the European Commission as part of the Marie-Curie-Initial Training Networks (ITN). Observations and multiproxy analysis are carried out at Istanbul Technical University (ITU), Eurasia Institute of Earth Sciences (EIES) and Eastern Mediterranean Centre for Oceanography and Limnology (EMCOL) laboratories. Palynological analysis is carried out in Faculty of Natural Sciences Department of Geology and Paleontology, Comenius University in Bratislava, Slovakia. The age model was constructed using AMS radiocarbon analysis in Beta Analytic Inc. North American Facilities.

Four major lithostratigraphic units have been identified in the BW-1 core section, along with a number of sub-units. This study provides around 7300 year high-resolution sedimentological record of using a multi-proxy approach of a sediment core from the Kızılırmak Delta Plain. Despite the limitations of a single core our results obtained from several methodologies (sedimentology, geochemistry and palynology) provide insights in the paleoenvironmental conditions.







# **KIZILIRMAK DELTASI'NDA SEDİMAN KAYITLARI, MULTİ-PARAMETRE YÖNTEMLER VE PALİNOLOJİ YARDIMIYLA PALEOORTAM YORUMLANMASI**

## **ÖZET**

Kızılırmak Deltası, Kızılırmak Nehri'nin Karadeniz'e döküldüğü yerde, taşıdığı sedimanlarla oluşmuş olup, Türkiye'nin kuzeyinde Orta Karadeniz Bölgesinde Samsun ili yakınlarında yer almaktadır. (41°30 to 41°45' N, 35°43' to 36°08' E).

Karadeniz'in son ana transgresyonu buzulların erimesine bağlı olarak, dünya çapında deniz seviyesinin yükselmesi ile doğrudan ilişkilidir. Son buzul döneminde aşınmış eski delta platformu seviyesine gelen Kızılırmak Delta platformunun doğu yakasının, buzullaşma sonrası dolmuş bir kanyon sisteminin parçası olduğu düşünülmektedir. Kanyonu dolduran sediman kaynağı Kızılırmak Nehri tarafından sağlanmıştır. Bu çalışmada, Kızılırmak Delta Düzlüğü doğu yakasında, bu dolmuş kanyonun bulunması beklenen lokasyonda bir sondaj çalışması yapılarak sediman karotu elde edilmiştir. Kızılırmak Nehri'nin yüksek sedimantasyon oranı, Kuvaterner çevre ve iklim koşullarına dair sürekli bir kayıt sağlamakta ve mükemmel bir arşiv oluşturmaktadır. Elde edilen sediman karotunda litolojik özellikler incelenmiş, multiparametre yöntemler uygulanmış ve palinolojik analizler gerçekleştirilmiştir. Ayrıca radyokarbon analizi ile yaş tayini yapılmıştır. Sediman karotunda farklı yöntemler uygulanarak kapsamlı veriler elde edilmiş, çapraz korelasyonlar yapılarak Kızılırmak Deltası paleoortam yorumları çıkarılmıştır.

Bu tez çalışması Avrupa Komisyonu tarafından desteklenmekte olan Marie-Curie-Initial Training Networks (ITN) kapsamında ve Anatolian pLateau climatE and Tectonic hazards (ALERT) projesi dahilinde yapılmıştır. Çalışmalardaki tüm gözlemler ve multiparametre yöntemler İstanbul Teknik Üniversitesi (İTÜ), Avrasya Yer Bilimleri Enstitüsü (AYBE) ve Doğu Akdeniz Oşinografi ve Limnoloji Araştırmaları Merkezi (EMCOL) laboratuvarları bünyesinde gerçekleştirilmiştir. Palinolojik analizler, Bratislava, Slovakya'da Comenius Üniversitesi laboratuvarlarında

yapılmıştır. Radyokarbon yaşlandırmaları için seçilen örnekler Kuzey Amerika'ya Beta Analytic Inc. laboratuvarlarına gönderilmiştir.

Kızılırmak sediman karotunda (BW-1) bir kaç ara birim ile birlikte temelde 4 ana lithostratigrafik birim belirlenmiştir. Bu çalışma, Kızılırmak Delta Düzlüğünde multi parametre yaklaşımlarla yaklaşık 7300 yıllık yüksek çözünürlüklü sedimantolojik kayıtları açığa çıkarmaktadır. Çalışmanın tek bir sondaj karotu ile gerçekleştirilmesinin sınırlayıcılığına rağmen, sedimantoloji, jeokimya ve palinoloji gibi farklı yöntemlerden elde edilen sonuçlar paleoortam yorumlanmasına katkı sağlamıştır.





## 1. INTRODUCTION

The Black Sea known is the world's largest, stable anoxic marine basin. The Kızılırmak Delta is the biggest and the richest wetland ecosystem in Black Sea Region comprising open water, marsh vegetation, sand dunes, farmland and remnant woodland. The Kızılırmak Delta is the delta of the Kızılırmak River and it is one of the most important deltas along the Central Black Sea Region of Turkey (41°30' to 41°45' N, 35°43' to 36°08' E). The Kızılırmak River is the longest river in Turkey (1355 km) that flows within Central Anatolian Plateau and eventually intersecting the delta and reaching into the Black Sea. The ecological system of the delta is extremely rich in terms of its biological variety as well as its fauna. The delta has been declared a Ramsar site, a wetland of international importance by the Ministry of Environment (Resmi-Gazete 1998) and covers an area of 50,000 ha that includes 15,000 ha of brackish marshes and swamps, coastal lakes, and lagoons and agricultural land (Özesmi, 1999).

This thesis was carried out in the context of Anatolian Plateau climate and Tectonic hazards (ALERT) project, funded and supported by the European Commission as part of the Marie-Curie-Innovative Training Networks (ITN) and carried out at Eurasia Institute of Earth Sciences (EIES), Istanbul Technical University (ITU). Within this large project, a sediment core was obtained from the eastern wetlands of Kızılırmak Delta plain. The main focus has been to reconstruct a paleoenvironmental development of the delta. By combining several techniques together, a high resolved Holocene development of the studied section of the Kızılırmak Delta has been revealed. During the laboratory analyses, different methods, such as sedimentological, geochemical and palynological analysis were used. These analyses consist of elemental profiling with X-Ray Fluorescence (XRF) Core Scanner, physical properties analysis with Multi Sensor Core Logger (MSCL), Palynological analysis and AMS radiocarbon dating.

## 1.1 The Black Sea Basin History

The Black Sea is an isolated inland sea, having limited interaction with the Atlantic Ocean and it is the largest anoxic basin in the world. There is a permanent oxic-anoxic boundary at around 100-150 m water depth that makes Black Sea oceanographically very interesting. The amount of Mediterranean inflow and velocity are the major controlling parameters of the oxic-anoxic boundary. Turkey's Black Sea coast contains three important deltas; Kızılırmak, Yeşilirmak, Sakarya. Sediments of Kızılırmak Delta provides high sedimentation rates that gives the opportunity to analyse changes of the oceanographic and environmental conditions since the Last Glacial Maximum (LGM, ~21000 BP) including the sea level, salinity, temperature, chemical, biological and climatic changes. Higher sedimentation rates give high-resolution paleoclimatic and paleoenvironmental development in a time range of Oldest Dryas to Holocene.

The latest major transgression of the Black Sea is related to the glacial melting accompanied with a worldwide sea level rise. There are evident from previous investigations that the Black Sea had been a fully isolated freshwater lake during the LGM and for some time after. The past estimations have uncovered that the most recent extreme ocean level rise happened in the early Holocene (~7500 BP) when the level of the Black Sea was 60 m beneath present ocean level. Subsequent worldwide ocean level rise brought about the Black Sea being suddenly associated with the Mediterranean Sea through the Dardanelles and the Bosphorus Straits and fast submergence around the Black Sea. Henceforth, the coastlines of Black Sea have encountered substantial changes in ocean level all through geological history. (Avşar, 2016)

## 1.2 Development of Kızılırmak Delta

The development of the Black Sea coast and delta is highly related to eustatic sea level changes, climatic changes and regional tectonic activity. The Kızılırmak Delta was studied in detail by Akkan (1970). According to his study Quaternary development of the Kızılırmak Delta has three levels (delta plains) that resulted because of climatically controlled regressions and transgressions. The first Kızılırmak Delta plain began forming during middle Pleistocene and the second around 100,000 years ago. The first two levels covers the largest area and comprise the slopes and higher altitudes of the delta, which presumably developed during Pleistocene high stands of the Black Sea when, as at present, it was connected to the Mediterranean Sea rather than forming an isolated lake basin. The third and the recent delta plain was formed during the Holocene by the alluvial sediments carried by the longest river (1355 km) of Turkey and its tributaries and eventually extended to the Black Sea. Recent delta plain also known the Bafra Delta Plain, includes numerous lagoons and wetlands formed by successional dunes and forests (Akkan, 1970; Ozesmi, 1999; Ozesmi, 1992). The age of delta sediments increases in inland direction, those of Holocene origin giving way to those of earlier Pleistocene (Banks and Thon, 1965).

The Holocene geomorphology on the Black Sea coast mostly developed under the control of climatic conditions. Changes in climatic conditions resulted in fairly rapid sea level rise of +2 m, (Flandrian transgression) from -40 m (Euxine regression) in sea level compared to existing level and at that period Black Sea level was 3-4 m higher than the recent level. The main geomorphological units of Kızılırmak Delta allow the distinct view of the traces of these sea level changes along the Black Sea coast during the Holocene.

Although Kızılırmak River is the most important source of delta build up, other streams from west to east; Alaçam, Gökçeboğaz, Betteş, Taşkelik, Ambarcıoğlu, Mera and Engiz have also contributed to its development. The local streams parallel to the Kızılırmak River feed the wetlands. The wetland area is parallel to the coastline on both sides of the delta. Eastern part of the delta incorporates an area of 13,400 hectares and has six lagoon lakes

(Liman, Balık, Uzun, Cernek, Gıcı, and Tatlı) and a western part that incorporates an area of 2,710 hectares containing Karaboğaz and Mülk lakes. The shape and formation of lagoon barriers are controlled by wind, waves, sediment influx from the rivers and longshore currents (Akkan, 1970; Ozesmi, 1992). The Kızılırmak riverbed is shallow which allows the water fluctuation greatly with the season, with a minimum in summer and maximum in spring. The climate of the area shows typical climate of the Black Sea. Warm-dry summers and mild-wet winters (Ozesmi, 1999). Average temperatures in January 6°C and 24°C in July.

### **1.3 Purpose of the Study**

There have been several different approaches taken to reconstruct sea level fluctuations throughout the Black Sea by using sediment cores. However, only few publications focus on our study area and the location of the sediment core obtained from the delta is quite important in terms of revealing sediment development of paleo delta depositional conditions. Consequently, this research aims to reconstruct in detail the paleoenvironmental conditions during the deposition of Kızılırmak, by combining sedimentological, geochemical, palynological and radiocarbon dating methods.



## 1.4 Literature Review

The Black Sea with its sedimentary archives represents a key location for palaeoclimate reconstructions. Black Sea was a freshwater lake isolated from the Mediterranean Sea during glacials (e.g. Schrader, 1979; Badertscher et al., 2011). Previous studies focused extensively on the last two glacial terminations on the Holocene climatic and environmental changes in the Black Sea (e.g. Ryan et al., 2003; Major et al., 2006; Bahr et al., 2008; Soulet et al., 2011; Shumilovskikh et al., 2013; Wegwerth et al., 2014). These studies revealed a generally strong response of the Black Sea to global sea level change. However, the post-glacial reconnection of Black Sea is highly controversial in scientific community. There have been two hypothetical flood scenarios proposed for the Black Sea. Ryan et al. (1997), proposed the so-called "Noah's Flood Hypothesis" where catastrophic seawater flood to a Black Sea freshwater at 7.15 ka BP leading researchers to examine Black Sea in detail. Ryan et al. (1997) found evidence of a massive flooding event at the Black Sea, by using core samples and determined that Black Sea was a freshwater body before flooding. Studies resulted in opposing interpretations (Aksu et al., 2002 and Ryan et al., 2014). Controversy over so-called Noah's Flood in the Black Sea comes from geological and foraminiferal evidence from the shelf. Other studies have been carried out to enlighten uncertainties that exist on the connection between the Mediterranean and Black Sea.

There have been several different approaches taken to reconstruct Holocene sea level fluctuations based on numerous sedimentological, geophysical, paleontological evidence and other methodologies and multi proxy analyses. (e.g. Demirbağ et al., 1999; Balabanov, 2007; Bahr et al., 2008; Ivanova et al., 2015). Studies resulted two opposing models a (semi-) catastrophic transgression within a very short term (e.g. Bahr et al., 2008) and long term with a continuous inflow up to 3.6 ka (e.g. Yanko-Hombach et al., 2014).

Between 1962–1973 more than 300 sediment samples revealed that the typical delta and seashore deposits of fine sand, sand, silt and silty sand alternations in the north of the delta belong to Quaternary (DSİ, 1986). Ardos, 1996; has explained the Quaternary development of the Kızılırmak Delta in a number of phases. Eustatic sea level changes played the important role of its formation, in both the glacial stages,

and in the interglacial stages. The delta shaped its present form after the Flandrian transgression, and the most important development was in the Holocene. Kuleli et al. (2009) developed an index to determine implications of sea level rise in Turkish coastal cities. Akkan, E. (1970); as part of his researches on geomorphology of the lower Kızılırmak, he has explained the Quaternary development of the ancient and recent delta and delta coastline of Kızılırmak River.

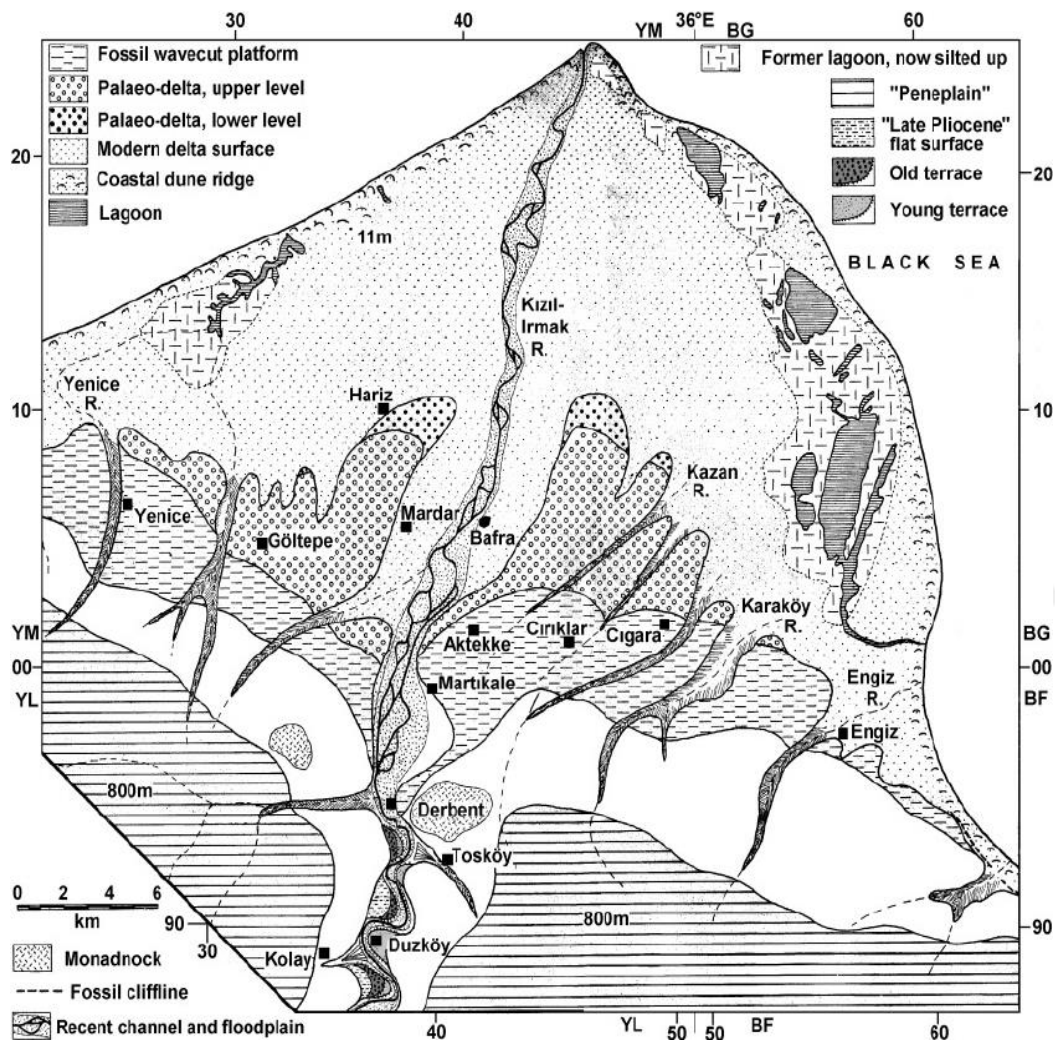


**Figure 1. Map of the lowermost reach of the Kızılırmak, showing the modern delta plain and two uplifted palaeo-deltas (Akkan 1970)**

## 1.5 Study Area

The Kızılırmak Delta is the biggest wetland area situated in the Central Black Sea region of Northern Turkey. Wetland area is mainly located at the eastern part of delta and this part is thought be part of a filled canyon system where sediments were supplied by the Kızılırmak River. The location for the drilling site was chosen by taking into consideration the possible location of filled canyon system. The coordinates of the site are between 41.57779 North latitude and 36.04755 East longitude, on the NE of the Kızılırmak Delta.

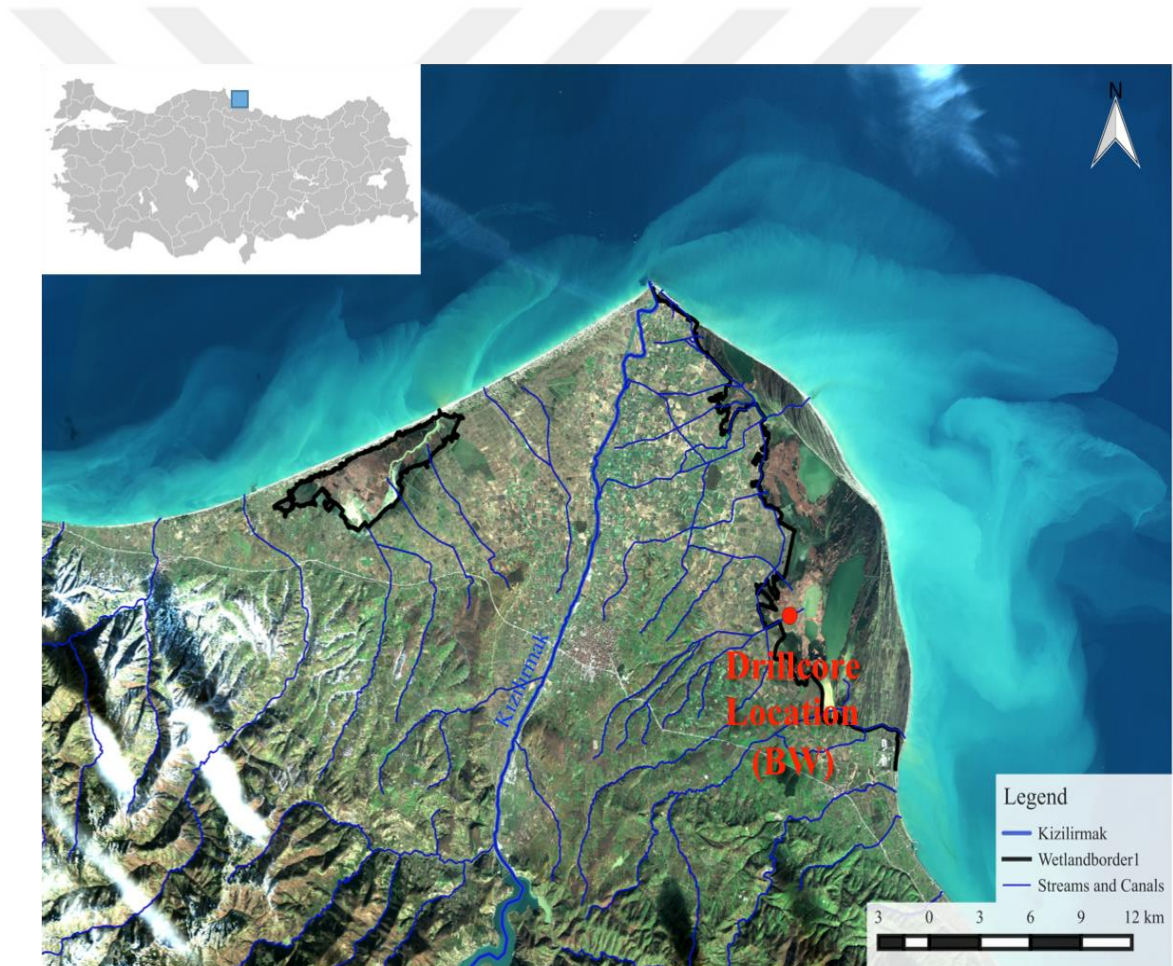


**Figure 2.** The Kızılırmak Delta study area, located at 41°34'40.0"N 36°02'51.2"E.

## **2. MATERIALS AND METHODOLOGY**

This study reports a combination of fieldwork in the study area and laboratory work in several lab facilities in İstanbul, Turkey and Bratislava, Slovakia. In this chapter, materials, equipments, lithological properties of the sediment core and analytical methods used to examine the core were explained. This study is funded and supported by the European Commission as part of the Marie-Curie-ITN project ALerT. Within the ALerT project two fieldworks took place in the study area. First fieldwork was carried out between 23<sup>rd</sup> June - 1st August 2015 to identify terrace sections and collect samples for Optically Stimulated Luminescence (OSL) dating of the fluvial strath terraces in order to understand regional tectonic uplift of the Central Pontides. However, this work is out of this thesis main subject. Second fieldwork for sediment coring was carried out between 15<sup>th</sup> October – 23<sup>rd</sup> October 2015. The sediment core BW\_1 (41.57779N, 36.04755E) was drilled down to 132 m below surface level (bsl) in the eastern Kızılırmak Delta plain and core sections with a diameter 76 mm of upper 32 m were collected from drilling site next to samples of lower 100 m. The bag sediment samples of lower 100 m were prepared for high-resolution micro faunal analysis. This part of work will be done within the ALerT project and it is also out of this thesis main subject.

### **2.1 Sediment Core and Sampling Methods**

A sediment core down to 132 m (with partial recovery) below surface level (bsl) has been drilled in the eastern wetlands of the Kızılırmak Delta plain. The upper 32 m was drilled with the mobile wire line drilling equipment and sampled in core boxes and lower 100 m was drilled with water and sampled in bags (one sample bag for each meter). All samples are collected and transported to Eurasia Institute of Earth Sciences, Istanbul Technical University. The first 32 m sediment core carried into splitting room at Eastern Mediterranean Centre for Oceanography and Limnology (EMCOL) of the Istanbul Technical University. Afterwards the core sections halved lengthwise for creating an archive half and a sampling half (also called working half)

by ITU EMCOL scientists. They are often called split cores. The archive half, was used for non-destructive physical properties estimations. It's called non-destructive because physical samples are not used for experiments that damage or destroy the sample contrary to working half (Rao, 2006). The working half was used for collecting samples for palynological analysis and radiocarbon dating. The archive half of the core was sampled in the middle part by U-Channels for the element profiling using the ITRAX XRF - Core Scanner and for physical properties by Multi Sensor Core Logger (MSCL). In March 2016, following XRF and MSCL analysis lithological description and facies interpretation has been done. A detailed description was recorded on the visual core description form ("barrel sheet") by using archive half and carried onto the Paleontological Stratigraphic Interval Construction and Analysis Tool (PSICAT) (CHRONOS 2006). 10 samples have been taken from the analysed samples for radiocarbon dating and 39 samples were collected for palynofacies analysis.

## **2.2 Sediment Description**

The description of sedimentary units was done on archive half right after non-destructive XRF analysis and physical properties analysis has been carried out. When the processes have been done with these equipments the split core was transported to sedimentology laboratory for Visual Core Description (VCD). Visual Core Description forms (also called barrel sheets) are completed for each section of each core. Barrel sheets are form that contain detailed visual description of sedimentology and summary of the stratigraphy, data for sedimentological units concerning their bed thickness, bed contacts, colour, grain size, lithology and sedimentary structures (Mazzullo and Graham, 1988). The sediment classification system used for this work depends on two types of observations; the macroscopic structure of the sediments (texture, colour etc.) and major-minor components of the sediments (clay, carbonate, mud, peat etc.) (Schnurrenberger et al., 2003). For colour-coding features Munsell Soil Chart was used. Combination of these data used for providing useful information about the paleoclimate and paleoenvironment.

The descriptions written manually on barrel sheets carried onto the Paleontological Stratigraphic Interval Construction and Analysis Tool (PSICAT) (CHRONOS 2006) for performing VCD's. PSICAT is very useful tool for scientist who wants to generate their own core description diagram. Generally, core description diagrams are drawn by hand and then carried onto graphics application like CoreDRAW. Paleontological Stratigraphic Interval Construction and Analysis Tool is a java based open source tool for creating and editing core description diagrams. The tool enables users to draw diagrams quickly and easily by creating some data, e.g., depth, grain size, and lithology automatically. Also, the data can be stored, making it accessible for changes or further analysis (Reed, 2007).

### **2.3 Gamma Density and Magnetic Susceptibility Analysis by Multi Sensor Core Logger (MSCL)**

Multi Sensor Core Logger (MSCL) tools are basically used to acquire non-destructive measurements along the length of the cores by using different sensors. They are designed to measure continuously and simultaneously, several physical properties such as magnetic susceptibility, gamma density, p-wave velocity and electrical resistivity.



**Figure 3. Geotek Multi Sensor Core Logger, MSCL**

MSCL devices allows users scan both whole core or split core up to 1.5 m long and 5 to 15 cm diameter with high resolution records. MSCL systems are widely used to provide quantitative data from sediment cores and measurements can be made accurately, rapidly, non-destructively and inexpensively (Geotek MSCL, 2016). In this study, split sediment core was sampled in the middle part by U-Channels for magnetic susceptibility and gamma density measurements. All measurements were carried out in Geotek Multi Sensor Core Logger (MSCL) equipment at the EMCOL laboratory in Istanbul Technical University. This equipment is essential for obtaining records of paleoclimatical and paleoenvironmental changes in cores. It is known that core-logging measurements vary extensively from in situ values due to release of overburden pressure and temperature changes during core recovery (Rothwell, 2006). It is taken into account that chosen drilling method might not give reliable results for p-wave velocity and electrical resistivity. Although this device is generally set up for various measurements, for this study, gamma density and magnetic susceptibility variations was recorded. The sediment core surface was covered with Mylar film in order to prevent moisture loss during measurements. Measurements completed with a resolution of 0.3 cm. The analytical results obtained from MSCL equipment are saved automatically using software based on “Windows” operating system. Graphs and formulas are created by the software, are used to evaluate the raw data (Geotek MSCL, 2016).



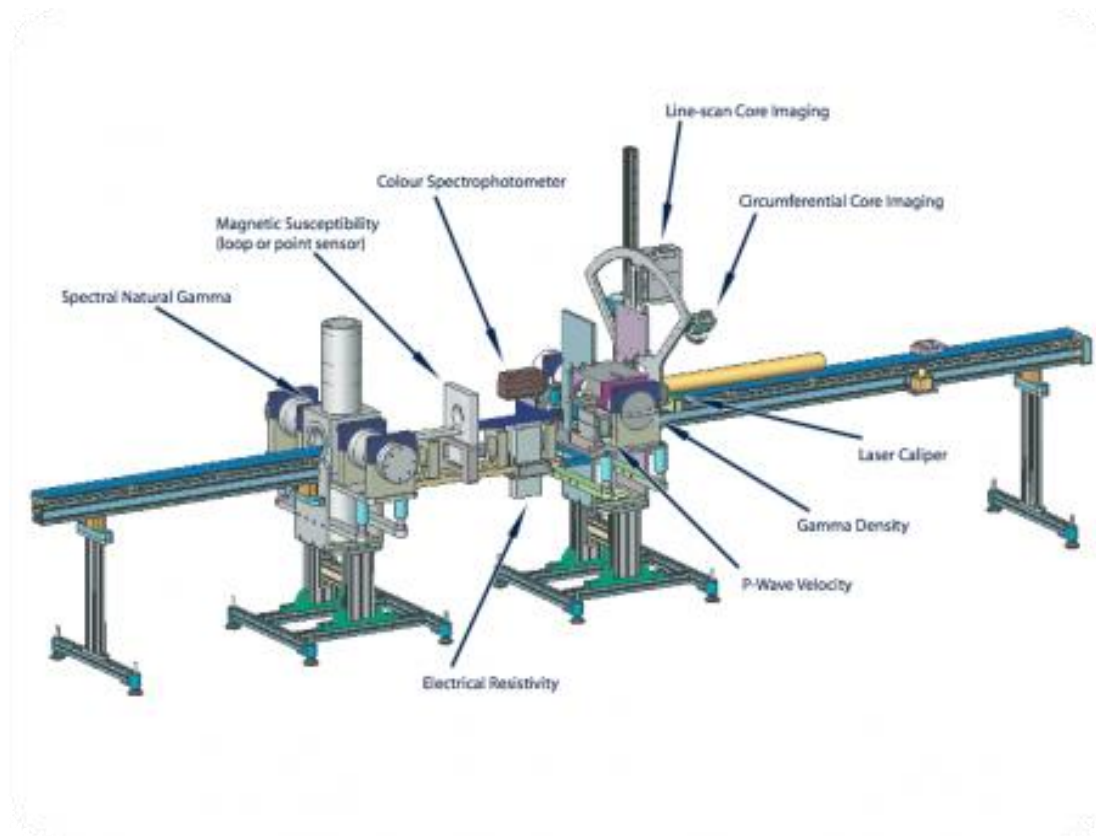


**Figure 4. Schematic diagram of a Geotek Multi Sensor Core Logger, MSCL**

### **2.3.1 Gamma Density**

Gamma density data can provide a precise and high-resolution record of bulk density, an indicator of lithology and porosity changes. Bulk density is usually measured using different techniques, so for MSCL the term gamma density is used. It is also called GRAPE (gamma-ray attenuation porosity evaluator) density. The measurement of gamma density is a widely used method and closely related to porosity, mineral and grain composition. The attenuation is directly related to core thickness and electron density. Measuring the number of transmitted gamma photons emitted by a beam through the core determines gamma density of the sediment core. A cylindrical material surrounded by water performs calibration of the measurement (Geotek MSCL, 2016).



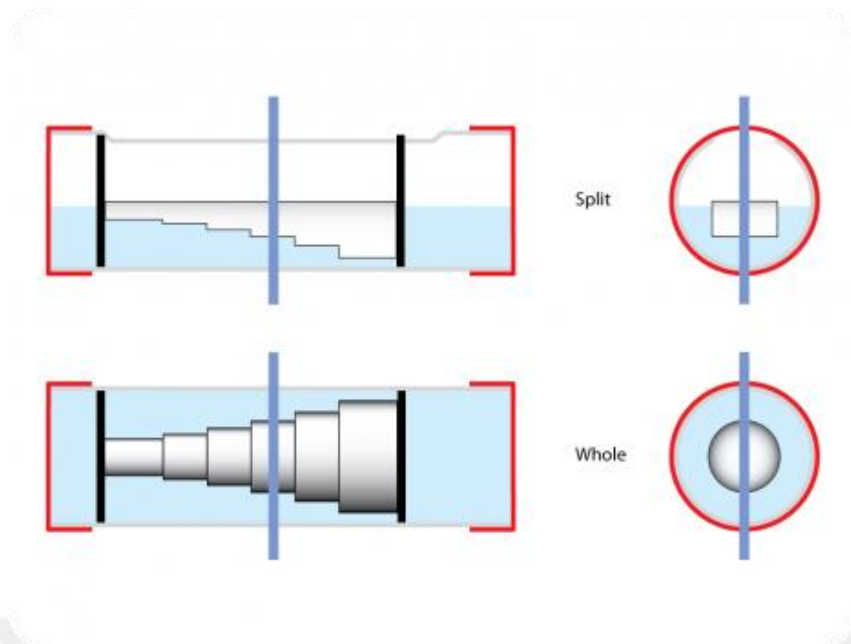


**Figure 5. Gamma density calibration materials**

### **2.3.2 Magnetic Susceptibility (MS)**

Magnetic Susceptibility is the ratio of magnetization of a material in response to an applied magnetic field. (Geotek MSCL, 2016) MS variations have been examined to identify sediment magnetic properties from the core that were recovered during drilling in the eastern Kızılırmak Delta plain. All magnetic susceptibility measurements were determined after the core was split in order to prevent magnetic mineral digenesis. Split core was analysed using Bartington point sensor (MS2E). Using this sensor high resolution, continuous, quantitative data of sedimentary records obtained from the core, which provides useful information for deriving potential paleoclimatic information. Magnetic susceptibility analysis conducted within the scope of this study has an important role in terms of showing terrestrial detrital input from sediment core. MS results are widely used for core correlation.

## 2.4 Element Profiling using ITRAX XRF-Core Scanner

The ITRAX XRF-Core Scanner provides X-radiographic images, optical image with an optical line-scanning camera and high-resolution elemental profiles of sediment cores and sediment u-channels using a flat beam X-ray sources (Croudace et al, 2006). Element Profiling using the ITRAX XRF-Core Scanner were carried out at the EMCOL Core Analysis laboratory in Istanbul Technical University.



**Figure 6. ITRAX XRF core scanner**

In the present study, the selected step size for U-Channels was 2.5 mm, counting for 10 seconds at each step, in order to analyse intensity of selected elements: Al, Si, P, S, Cl, Ar, K, Ca, Sc, Ti, V, Cr, Mn, Fe, Co, Ni, Cu, Zn, Ga, Ge, As, Se, Br, Rb, Sr, Y, Zr, Nb, Mo, Cd, Sb, I, Cs, Ba, La, Ce, Hf, Ta, Pb, THz, U. In order to obtain reliable results sandy sediments were avoided.

## **2.5 <sup>14</sup>C Dating of the Sedimentary Sequence**

Accelerator Mass Spectrometry (AMS) detects the naturally occurring radiocarbon isotope (<sup>14</sup>C) to estimate the age of the several materials (such as shells, peat, wood etc.) up to about 58,000 to 62,000 years (Plastino et al., 2001). Chronology of the core was determined by a radiocarbon dating. Accelerator mass spectrometry is an advanced radiocarbon dating method that is considered to be the more effective approach to measure radiocarbon content of a sample (Grice, 2015). Significant stratigraphic features were targeted for dating to produce chronology. Samples were taken at certain depths along the sediment core and sent to Beta Analytic Inc. North American Facilities for sample preparation and Accelerator Mass Spectrometry analysis. Total 9 samples with weight of > 10 mg were taken carefully by using metal knife and packed with aluminium foil for avoiding contamination of the samples. Handling the samples with bare hands in organic matters would contaminate the samples, because of modern oils present in hands. Chemical preparation employed by Beta labs for all types of samples that were measured by accelerator mass involving washing the shells with dilute hydrochloric acid (HCL).

## 2.6 Palynological Analysis

Palynological analyses are a great tool for useful information on depositional environments. For palynological analysis, 38 samples were studied in total. The depth range of the samples between 0 to 32 m depths bsl. For this analysis samples were taken along the sediment core by using plastic spoons and metal knives, and collected in geochemical sample bags and transported to Faculty of Natural Sciences Department of Geology and Paleontology, Comenius University in Bratislava, Slovakia. Sediment samples were prepared according to the laboratory procedures. Preparation of the palynological samples was done according to standard method (Cour, 1974). Twenty grams dry sediments were taken for each of samples. In order to calculate palynomorph concentrations two *Lycopodium clavatum* tablets was added to each of the sediment samples (Stockmarr, 1971). Then %35 hydrochloric acid (HCl) was added to dissolve carbonates within the samples and left to settle overnight. The day after all samples was then centrifuged until the samples were cleaned. Then %35 hydrofluoric acid (HF) was added to dissolve silicates within the samples. Two days after all samples were centrifuged until the samples were cleaned. For oxidation the samples were treated with HCl once again. Afterwards heavy liquid (ZnCl<sub>2</sub>) was applied and left until pollen circle appear on the top part. Mixes of glycerol and pollen fraction were mounted on microscope slides. Adding glycerol into pollen fraction allows rotation of pollen grains that improves their examination and identification using light microscopy.

### 3. RESULTS

In this chapter, all results of the analysis are given. First part of this chapter includes the detailed lithostratigraphy and chronostratigraphy results of the sediment core from 0 to 12.18 m bsl  $\approx$  30 m bsl. Further on this chapter, physical properties measured by MSCL, elemental profiling results using ITRAX XRF Core scanner and palynological results are given in an order.

#### 3.1 Lithostratigraphy and Chronostratigraphy

In this section cores recovered from Kızılırmak Delta plain and recorded on the VCD forms showing their lithological properties are summarized. Individual sediment units were identified and logged for colour, structure, grain size, and presence of shell, organic matter and other accessories. Created logs are carried onto the Paleontological Stratigraphic Interval Construction and Analysis Tool (PSICAT) (CHRONOS 2006).

- Lithological description and radiographic image of the sediment core 1 m bsl shown Figure 7.

The uppermost 0,26 m of the core shows a dark grayish brown colour mud with small iron oxide dots. On top of the interval around 0,03 m black cultured wedge was recognized. From 0,26 m of the core until the 0,645 m the colour of the material changes progressively from dark grayish brown to olive brown. Both upper and lower contacts are indistinct. Interval consists oxidized brown patch and iron oxide dots. 0,645 - 0,715 m interval is dark gray mud with shell fragments. 0,715 to 0,775 m interval is olive brown colour and has same material as interval 0,26 - 0,645 m. From 0,645 to 0,825 m coarser grain size and darker colour is observed. Around the interval 0,82 to 0,83 m light olive brown wedge shape material is observed. 0,825 to 0,93 m interval shows very dark gray mud with small iron oxide dots. From the top of the core until the depth of 0,93 m interval shows muddy fine sand, soil structure. From top to bottom of the first meter of a sediment core shows shell fragments only at 0,645 - 0,715 m interval. Below 0,93 m core depth material becomes very dark gray organic rich mud with wood pieces.

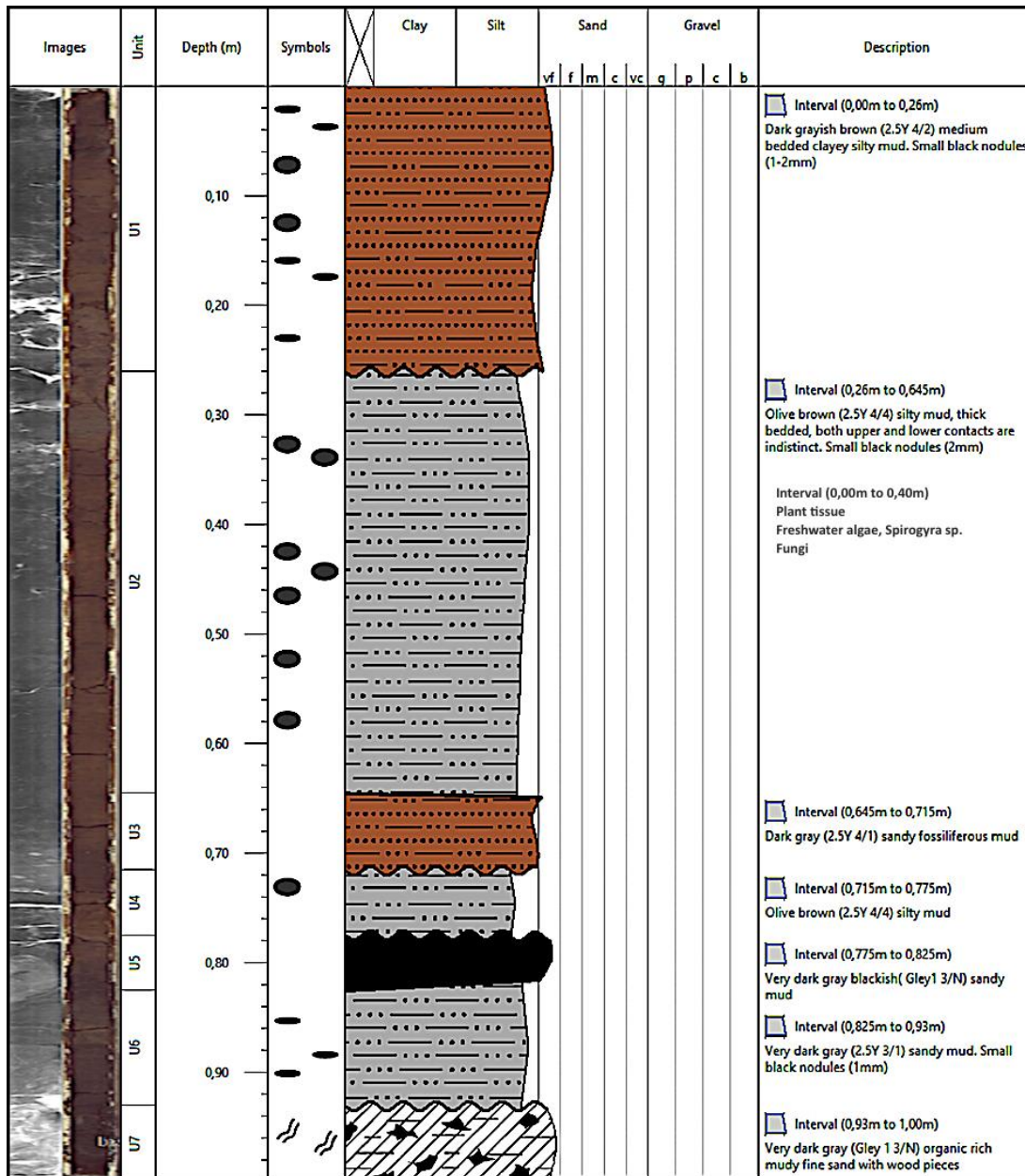


Figure 7. Digital photography, radiographic image and lithological description of the sediment core from 1 m bsl.

- Lithological description and radiographic image of first meter of the sediment core from 1 m to 2 m below surface bsl shown in Figure 8.

1 to 1,45 m of the core interval is very dark gray mud with oxidized brownish patch and iron oxide dots. This interval starts a 0,93 m of the core but from 1 m no wood pieces observed. Around the interval 1,081 to 1,091 m reddish brown half laminae observed. The interval consists light gray brownish oxidized interbeds between 1,325 - 1,365 m and 1,399 - 1,411 m. From 1,45 m to 1,8 m interval shows black coloured organic rich mud with wood particles. At 1,8 - 1,96 m core depth the colour of the mud changes into dark gray and it consist brown oxidized patches. Below this interval until 2 m no sediment recovered.



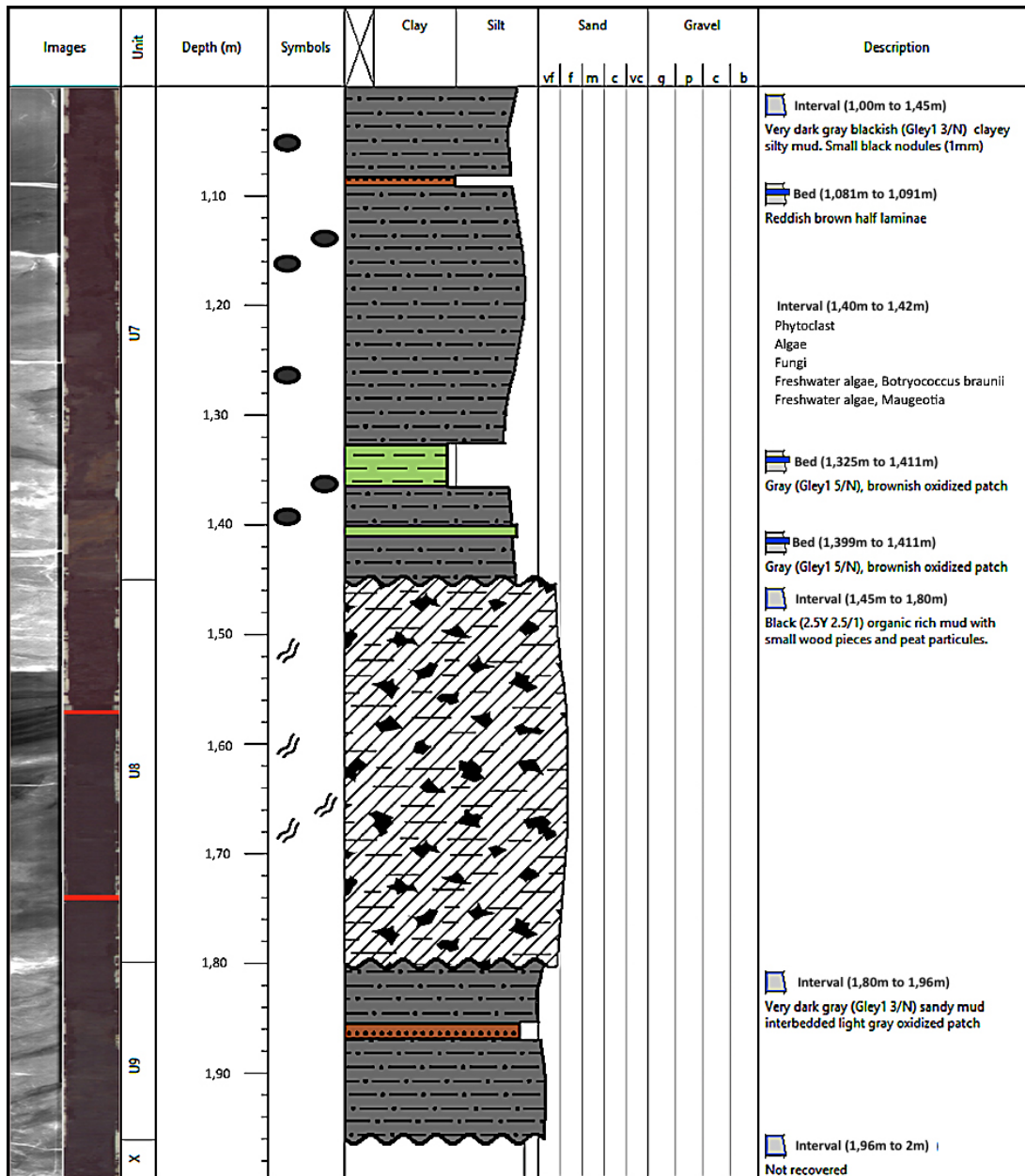


Figure 8. Digital photography, radiographic image and lithological description of the sediment core from 1 m to 2 m bsl.



- Lithological description and radiographic image of first meter of the sediment core from 2 m to 3 m below surface bsl shown Figure 9.

This part of the core sediments from 2 m to 3 m are changes in colour from dark gray to olive gray respectively. First interval of this sediment core depth at 2 m to 2,07 m is dark gray mud. Below this interval until the depth of 2,15 m mud changes its colour to lighter gray and it consists oxidized brownish patches. From 2,15 m to 2,20 m material is darker gray. Between the core depths of 2,20 m to 2,26 m material colour changes again to olive gray with oxidized brownish patches. At 2,26 m to 2,43 m core depth interval colour is light olive brown, oxidized brownish patches continuous and consists iron oxide dots. At around 2,345 m black wedge shape mud was recognized. Between 2,43 m to 2,45 m sediment core is not recovered. Following interval from 2,45 m to 2,59 m consist same colour and material as interval 2 - 2,07 m and 2,20 - 2,26 m. From 2,59 to 2,64 m interval colour changes to very dark gray. At around 2,60 m light red coloured pottery piece observed. 2,64 - 2,69 m interval shows olive gray mud lithology without any oxidation indication. From 2,69 m to 2,95 m interval shows very dark gray to black colour. Sediment consists of small iron oxide dots. Interval shows same lithology as interval 1- 1,45 m. Below 2,95 m of this core section is olive gray mud showing same lithology as interval 2,45 - 2,59 m. This interval ends at 3,24 m. No shell or shell fragments are observed from this core section.

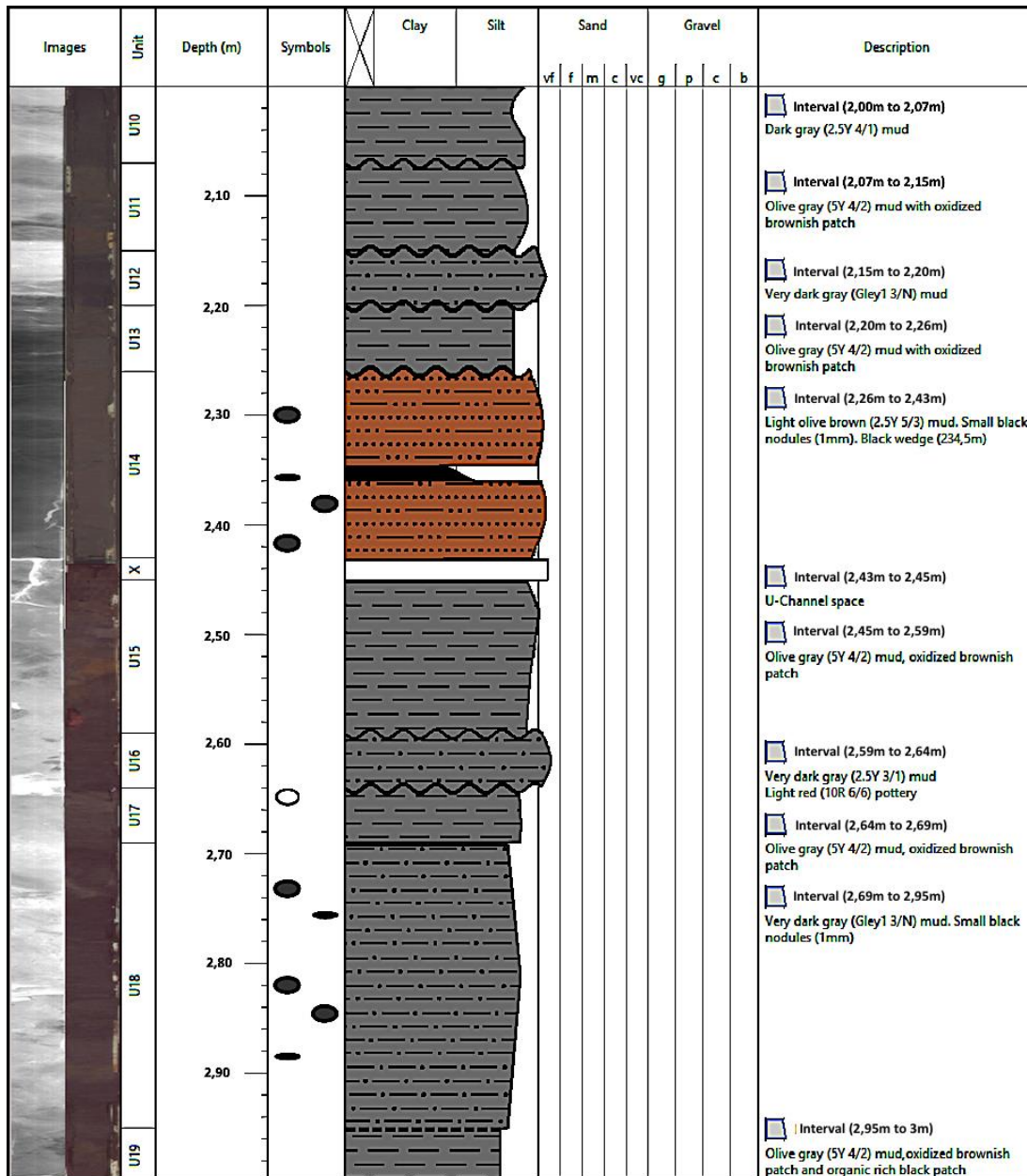
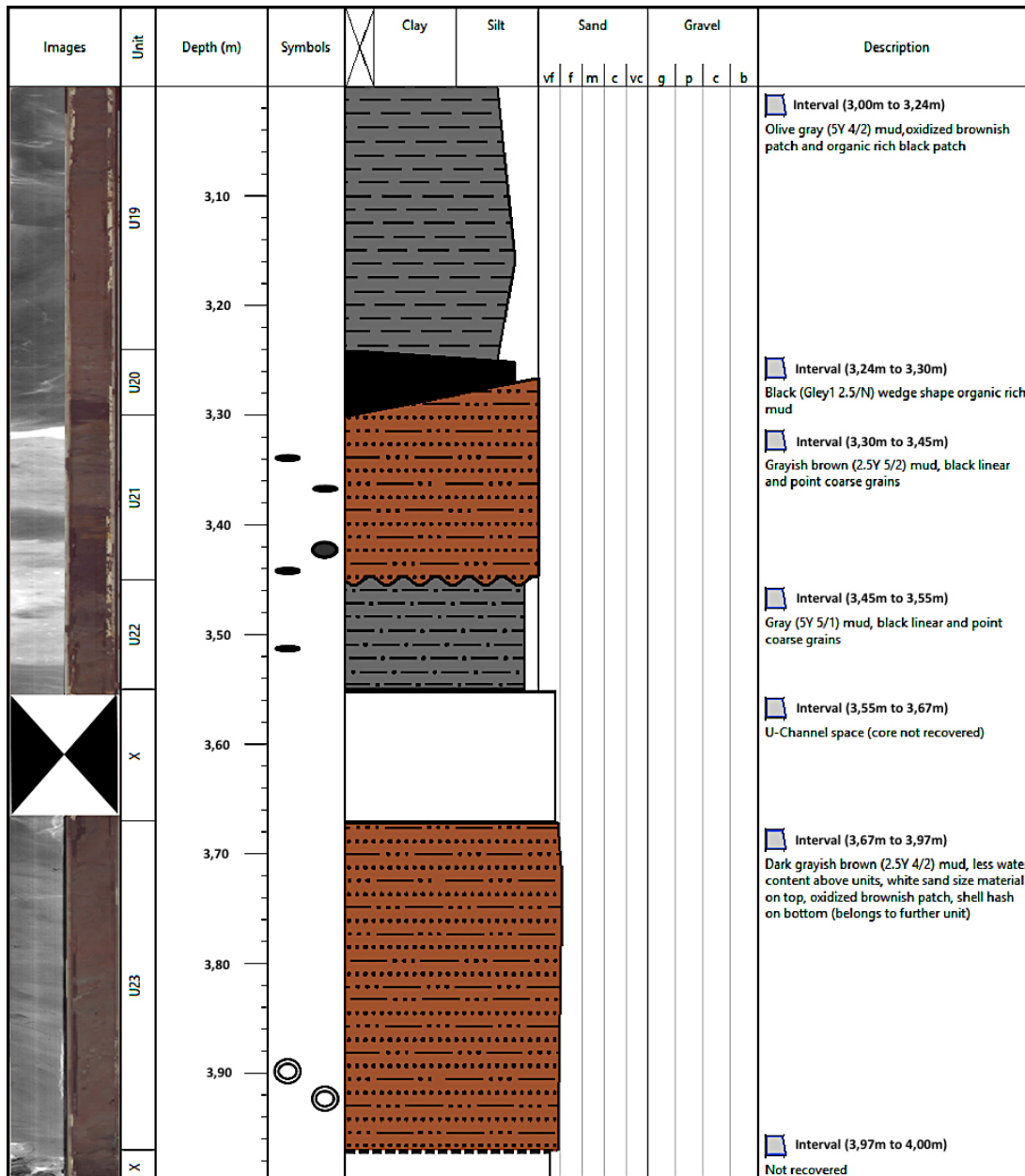


Figure 9. Digital photography, radiographic image and lithological description of the sediment core from 2 m to 3 m bsl.

- Lithological description and radiographic image of first meter of the sediment core from 3 m to 4 m bsl shown Figure 9.

First interval for this section start from at 2,95 m and it ends at 3,24 m. This interval is olive gray mud showing same lithology as 2,45- 2,59 m and it consist oxidized brownish patch as well. In between intervals of 2,95 - 3,24 m and 3,30 - 3,45 of the core section consist black coloured wedge shaped organic rich mud observed. Below this organic rich mud colour changes to grayish brown and grain size becomes coarser. This interval consists small point and linear grains on top. From 3,45 m to 3,55 m colour shows a progressive change from grayish brown to gray, although lithology remains the same. At 3,45 - 3,67 m depth no sediment recovered. Below 3,67 m there is a sharp lithological change. This interval shows dark grayish brown mud with white sand size material on top and oxidized patches. The water content of this interval is less than above units. A shell layer that possibly belongs to units recognized at the bottom of this interval is also present. No shells are visible except this layer along the interval. Below 3,97 m until 4 m no sediment could be recovered.



**Figure 10. Digital photography, radiographic image and lithological description of the sediment core from 3 m to 4 m bsl.**

- Lithological description and radiographic image of first meter of the sediment core from 4 m to 5 m below surface bsl shown Figure 11.

The uppermost 0,13 m is homogeneous light greenish gray mud without some shell fragments. This interval has less water content as in interval 3,67 - 3,97 m. From 4,13 m to 4,25 m depth sediment consists very dark greenish gray sandy mud with large and whole shells. Following interval at the depth of 4,25 to 4,35 m is greenish gray sandy mud without any shell or shell fragments. This core section consists 3 intervals without sediment recovery at the depths of 4,35 - 4,37 m, 4,50 - 4,53 m and 4,69 - 4,72 m. At 4,37 - 4,5 m depth very dark greenish gray as in 4,13 - 4,25 m interval is observed. However, this interval consists only of small shells. Between 4,53 m and 4,88 m core depth material again becomes greenish gray dominated by large shell fragments. From 4,88 to 5,44 m of the sediment core shows dark greenish gray fine sandy mud with shells and shell fragments (Figure 10, 11).

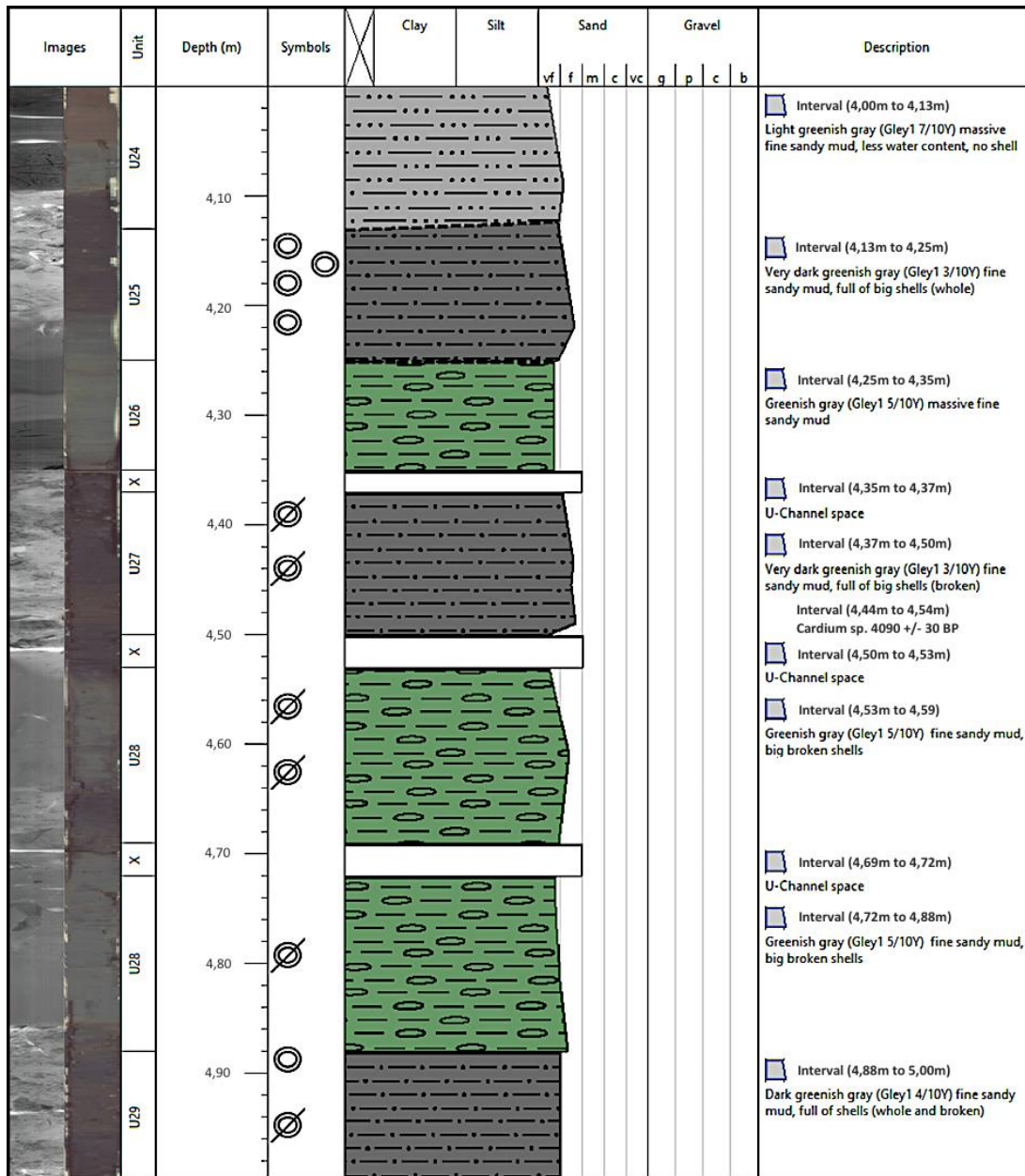


**Figure 11. Digital photography, radiographic image and lithological description of the sediment core from 4 m to 5 m bsl.**

- Lithological description and radiographic image of fifth meter of the sediment core from 5 m to 6 m bsl as shown Figure 12.

This core section starts with the same lithology as in 4,88 - 5 m. Although there is no lithological change along this core section, there are levels with dense mollusc population. Figure 11 shows a lithological column that starts from 5 m to 5,44 m dark greenish gray fine sandy mud with shells and shell fragments. From the 5,44 m of the core until the bottom of the core section lithology and colour remains the same, however this interval consists of less dense and broken shells. Between 5,815 m and 5,835 m no sediment core was recovered.



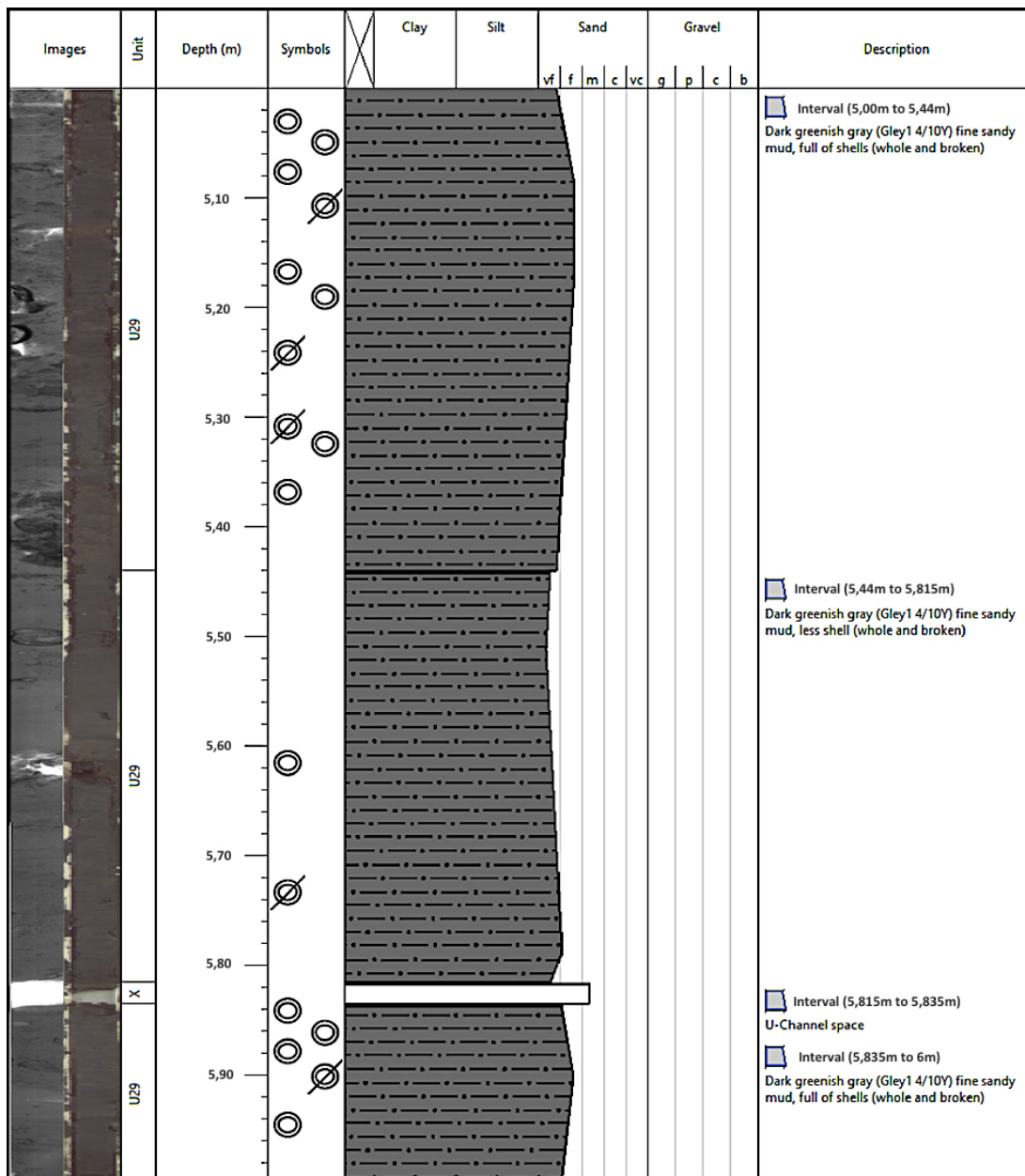


**Figure 12. Digital photography, radiographic image and lithological description of the sediment core from 5 m to 6 m bsl.**



- Lithological description and radiographic image of fifth meter of the sediment core from 6 m to 7 m below surface level (bsl) shown Figure 13.

There is no lithological change along this core section. Levels with dense mollusc population and storm events are observed at some layers. The uppermost 0,09 m of this core section shows same lithology, as above unit and it is dark greenish gray fine sandy mud with less dense mollusk population. At around 6,03 to 6,04 m thin shell hash layer observed. From 6,09 m to 6,49 m whole and broken shells are abundant. Between 6,49 m and 6,70 m interval shows same lithology, dense mollusc population, however all shells are mm scale and broken which indicates a catastrophic event possibly a storm. Two thin layers consisting very small shell hashes are observed at the depth of 6,51 - 6,52 m and 6,54 - 6,55 m. Between 6,70 and 6,71 m interval no sediment was obtained from the core. From 6,71 m to 7 m (until the end of the core section) whole and broken shells become abundant again.

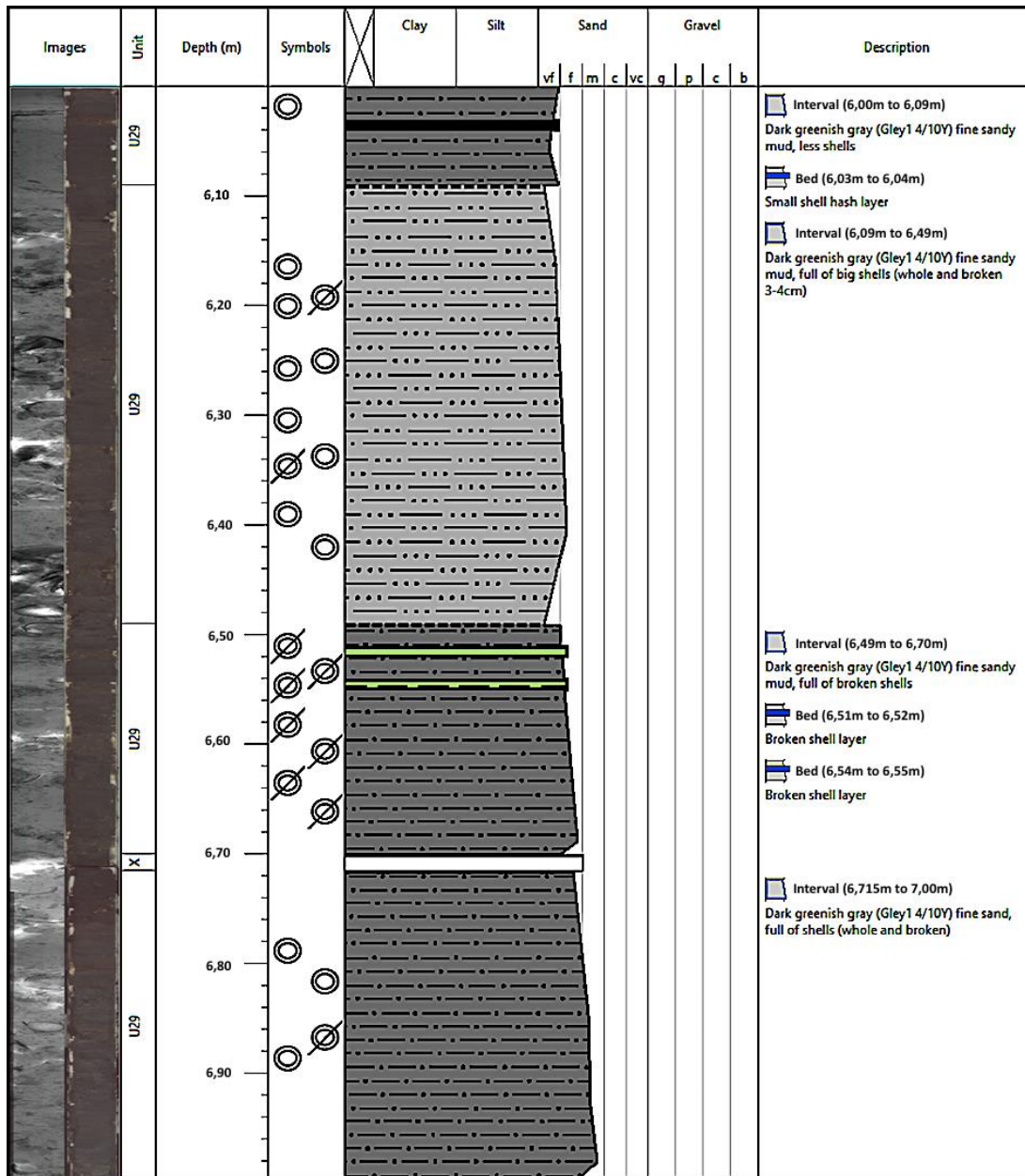


**Figure 13. Digital photography, radiographic image and lithological description of the sediment core from 6 m to 7 m bsl.**

- Lithological description and radiographic image of fifth meter of the sediment core from 7 m to 8 m bsl shown in Figure 14.

This core section from 7 m to 8 m shows same lithology as in the upper unit and it is dark greenish gray fine sandy mud with full of shells. Radiographic image shows the density changes and the shell content throughout the core. Upper half of the sediment core shows much more shell content.

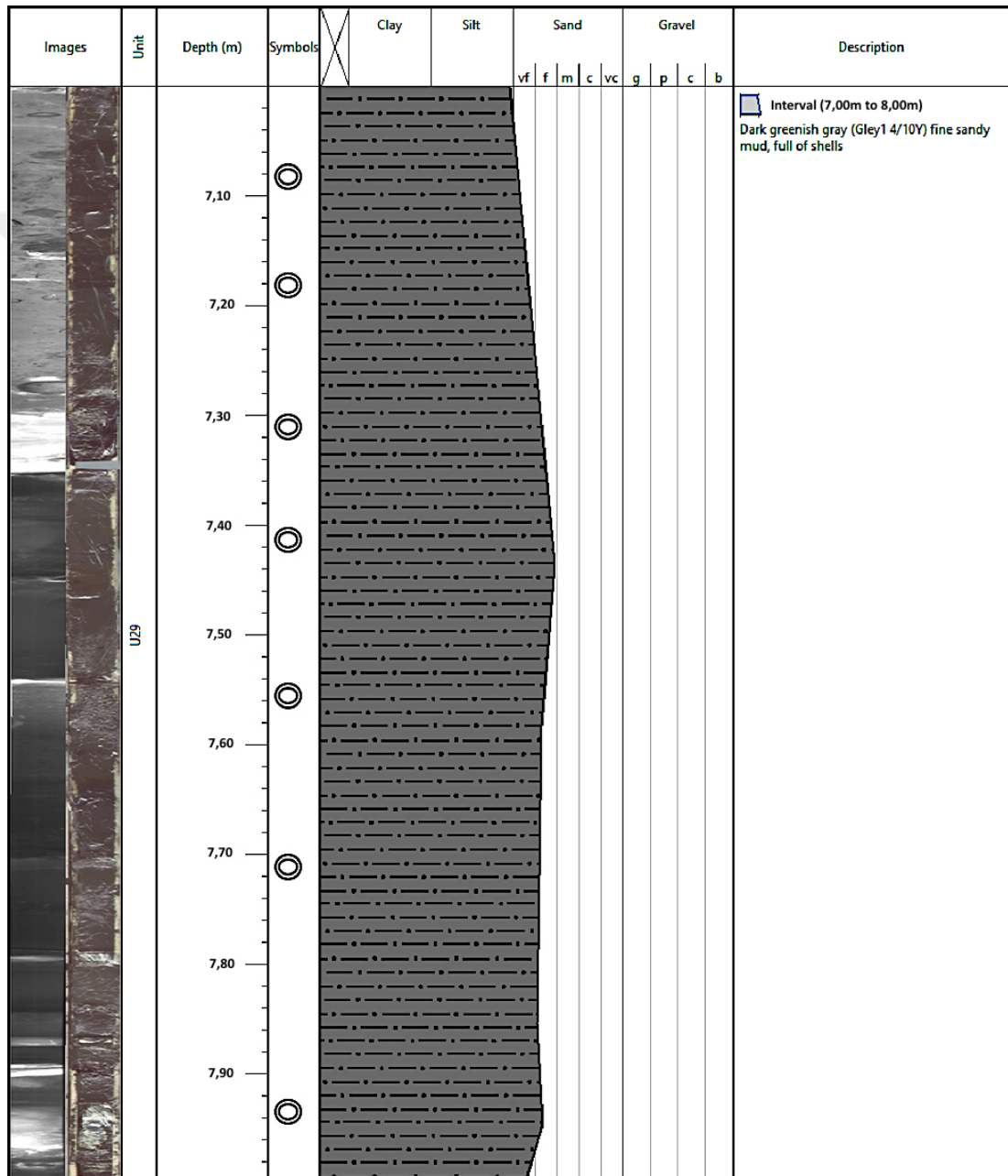


**Figure 14. Digital photography, radiographic image and lithological description of the sediment core from 7 m to 8 m bsl.**

- Lithological description and radiographic image of fifth meter of the sediment core from 8 m to 9 m below bsl shown in Figure 15.

Uppermost 0,33 m of the sediment core section shows same lithology as in above unit, however material become coarser from 8,07 m. This unit also consists of shells and shell fragment as above unit. From 8,33 m to 8,50 m interval colour becomes lighter and consists mostly of whole shells and relatively less shell hashes. Following unit from 8,50 m to 8,59 m shows an abrupt lithological change. The interval consists very dark gray organic rich mud with small amount of shell fragments. Inside the interval at around 8,51 m dark brown linear patch observed. Between 8,59 m and 8,62 m interval no sediment obtained from core. Below 8,62 m material colour progressively changes its colour into lighter gray. Interval between 8,62 to 8,95 m shows olive gray muddy sand with small iron oxide dots. At 8,76 m large and whole shell is recognized. From 8,95 to 9 m interval consists of olive gray disturbed medium size sand.

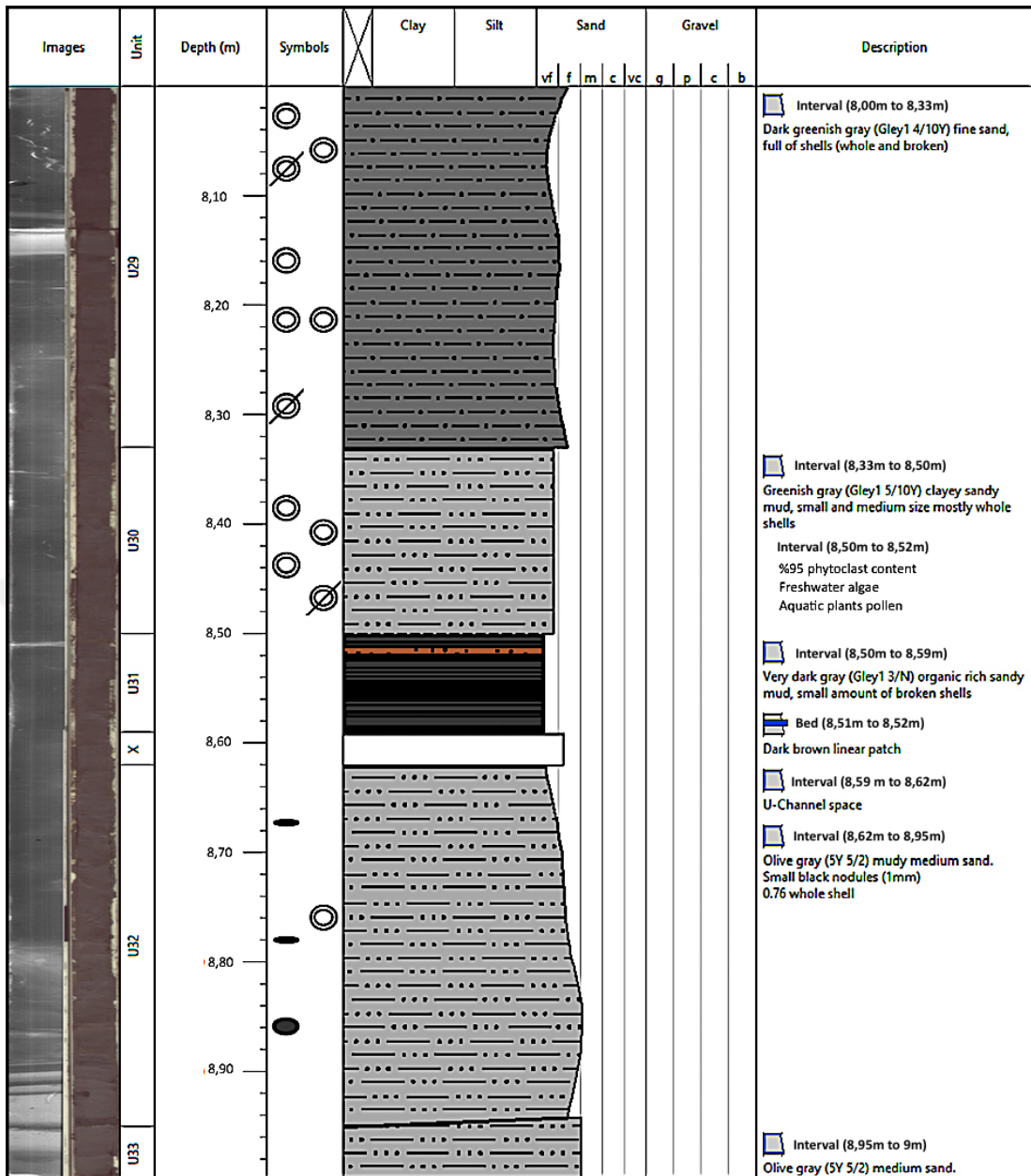


**Figure 15. Digital photography, radiographic image and lithological description of the sediment core from 8 m to 9 m bsl.**

- Lithological description and radiographic image of fifth meter of the sediment core from 9 m to 10 m bsl shown in Figure 16.

There is no sediment recovery at the uppermost 0,05 m of the core section. From 9,05 to 9,20 m interval shows greenish gray muddy sand consisting very small and in small quantities shell fragments. At around 9,15 to 9,17 m black coloured wedge shape patch was recognized. Occasionally small iron oxide dots are observed. Below the sharp boundary at 9,20 m until 9,33 m depth, colour of the material changes into darker gray and it consists of relatively small shell fragments. Following interval from 9,33 to 9,49 m, is composed of greenish gray mud and in small quantities sand. At the bottom of the interval oxidized brownish patches and big size broken shells are observed. Interval shows relatively darker layers with same material from place to place. Below 9,49 m interval until 9,61 m colour of the material become lighter and it consists very small iron dots and shell fragments. At around 9, 57 m and at the bottom of the interval darker colour sand layers are observed. From 9,61 m to 9,75 m interval shows dark greenish gray sandy mud. This unit consists of black colour wedge shape peat and some shell fragments. Below 9,75 m until the bottom of the unit shows again dark greenish gray muddy medium sand and it consists of some shell fragments.

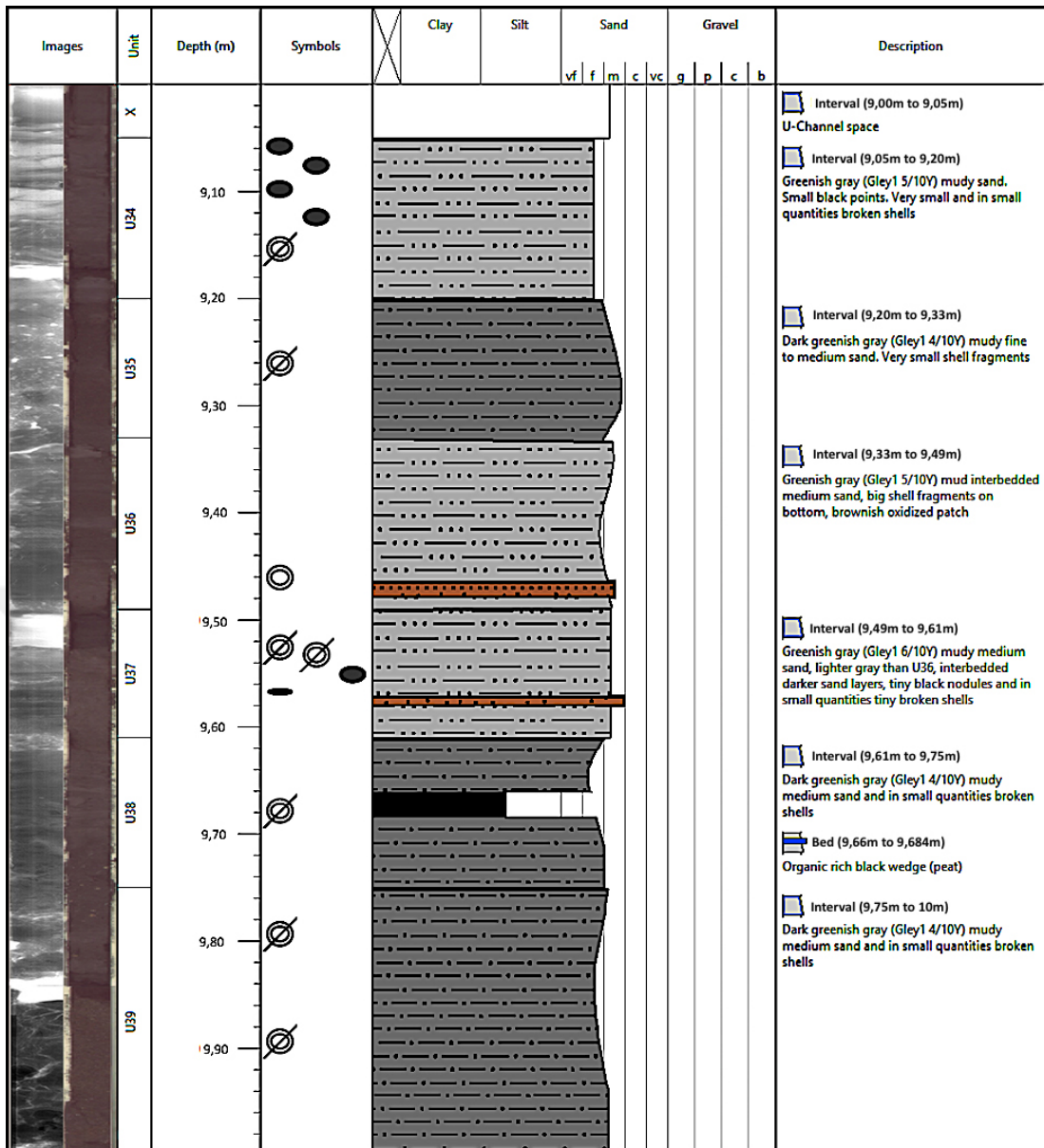


**Figure 16. Digital photography, radiographic image and lithological description of the sediment core from 9 m to 10 m bsl.**

- Lithological description and radiographic image of fifth meter of the sediment core from 10 m to 11 m below surface level (bsl) shown in Figure 17.

Upper 0,03 m of the sediment core shows greenish gray clayey sand. From 10,03 m to 10,76 m of interval sediment has a colour of dark greenish gray. Material is fine to medium sand and there are no shells and shell fragments between these depths. From 10,76 m to the end of the core section, material shows grayish brown colour fine sand consisting of clayey medium sand layers.

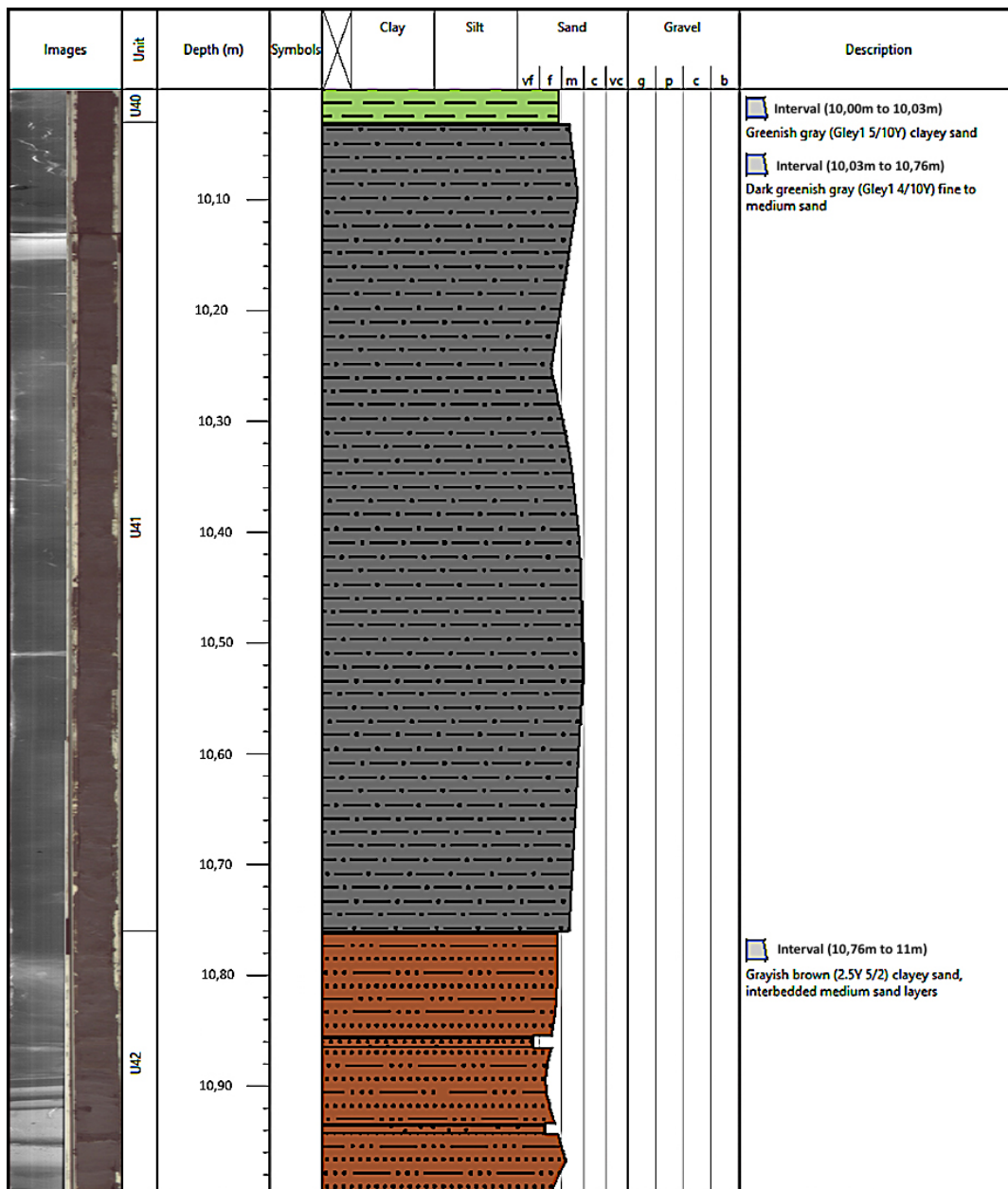


**Figure 17. Digital photography, radiographic image and lithological description of the sediment core from 10 m to 11 m below surface level**



- Lithological description and radiographic image of fifth meter of the sediment core from 11 m to 12 m bsl shown in Figure 18.

Uppermost 0,17 m of this core section shows same lithology as above unit. Colour of the sediment is grayish brown and it shows fine sand interbedded clayey medium sand layers. Following interval from 11,17 m to 11,41 m show same lithology however, interbeds shows fine sand. From 11,41 to 11,43 m interval shows lighter colour sand without any clay content. At the 11,43 - 11,54 m interval shows grayish brown clayey medium sand. Following unit from 11,54 m to 11,56 m shows same colour as interval 11,41 to 11,43 m. Next interval 11,56 m to 11,62 m shows again grayish brown colour clayey sand. There is a small interval from 11,62 m to 11,65 consisting lighter brown colour sand without any clay content. Below 11,65 m until 11,85 m interval shows grayish brown sand. Interval is composed of large shell fragments. From 11,85 m until the end of the sediment core colour becomes lighter. Interval shows light brownish gray medium size sand consisting shell fragments.

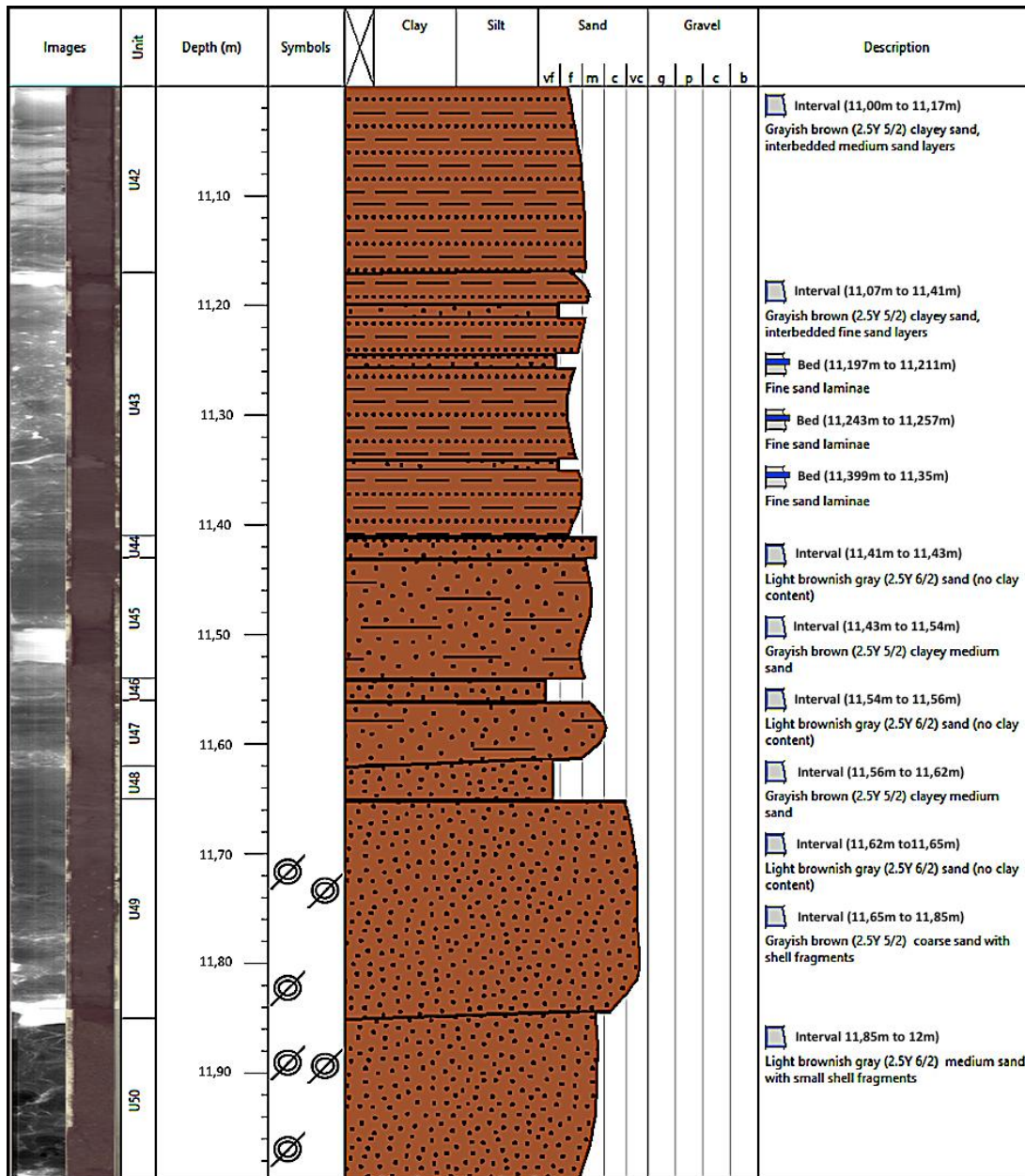


**Figure 18. Digital photography, radiographic image and lithological description of the sediment core from 11 m to 12 m bsl.**

- Lithological description and radiographic image of fifth meter of the sediment core from 12 m to 13 m bsl shown in Figure 19.

From top to bottom of this core section (12 m to 13 m) shows dark grayish brown colour medium size massive sand. This interval consists of small quantities shell fragments. There is no radiographic image obtained for this core section.

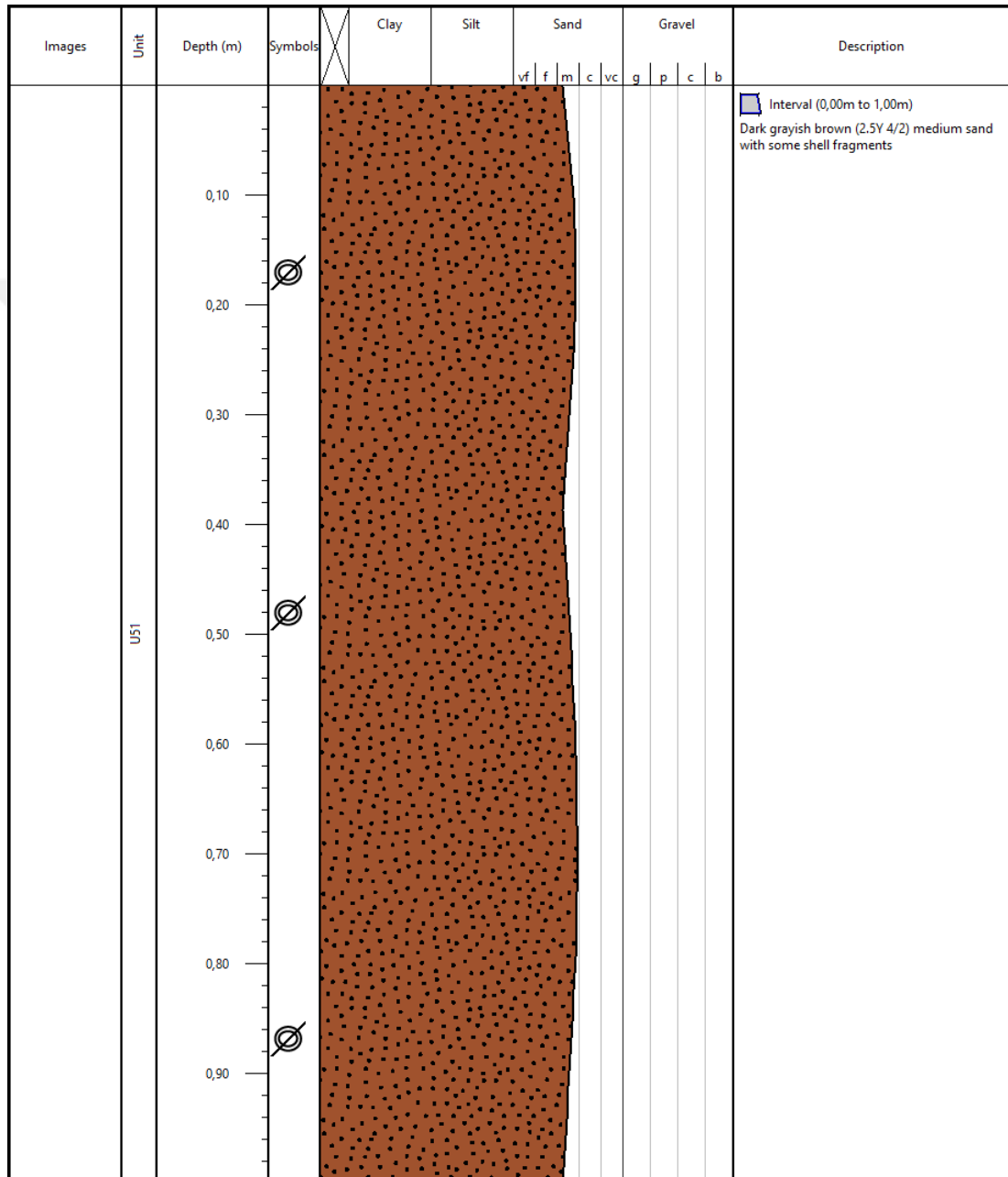


**Figure 19. Digital photography, radiographic image and lithological description of the sediment core from 12 m to 13 m bsl.**

### 3.2 MSCL RESULTS

In this section gamma density and magnetic susceptibility results measured by MSCL device are given in detail. Core sections are put together as one whole core and measurements are given in one diagram. Gamma density values are given as  $\text{g/cm}^3$  and magnetic susceptibility values are given as SI unit. The whole core gamma density, fractional porosity and magnetic susceptibility records are shown in Figure 20.

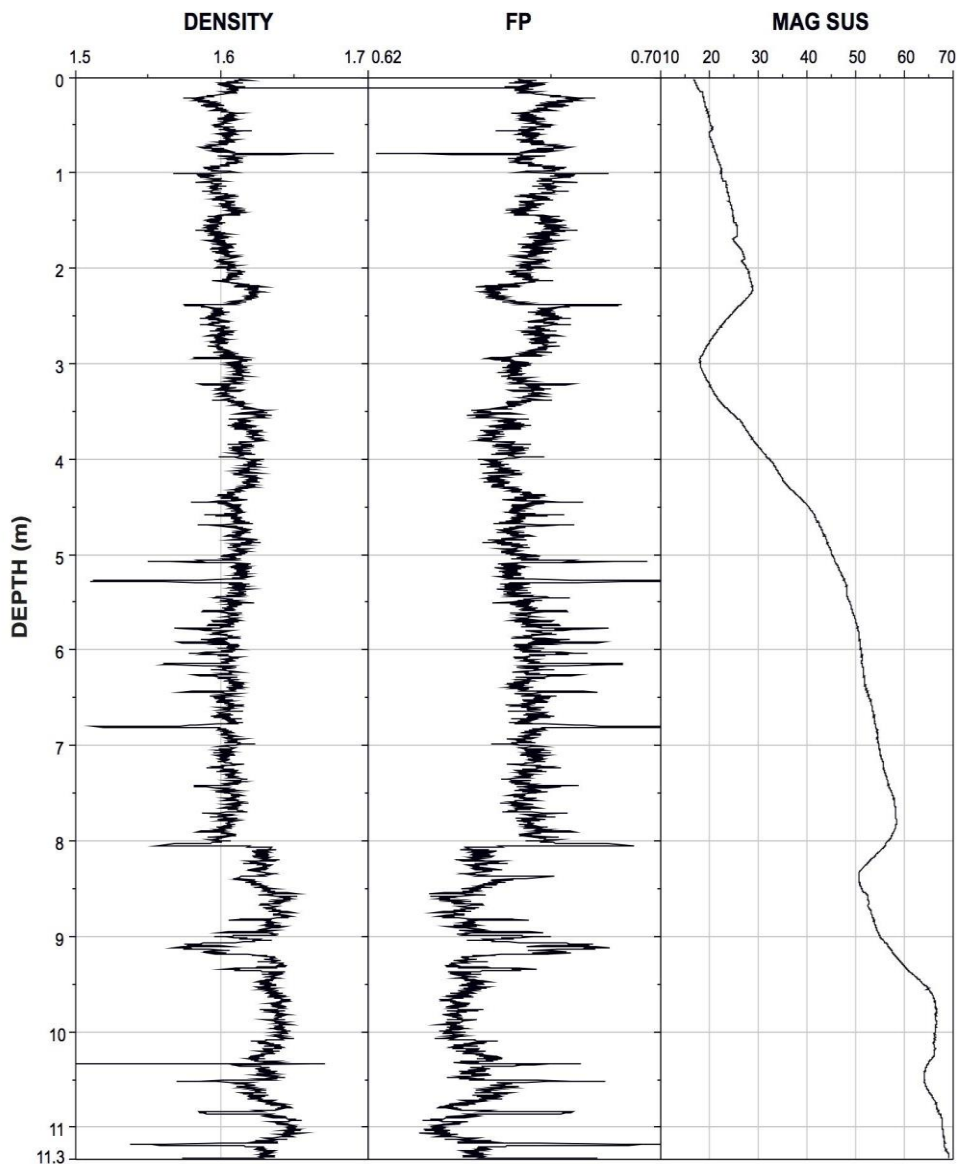


**Figure 20. Gamma density, fractional porosity and magnetic susceptibility results**

Magnetic susceptibility of the topmost part of the core shows distinct increase until the 2,2 m core depth indicating terrestrial input and accumulation of iron rich material. Gamma density values fluctuate indicating the lithological changes of the core section. Higher gamma density values correspond to lower fractional porosity values throughout the core length. Following interval shows an abrupt decrease until 3 m of the core length. The distinct changes of magnetic susceptibility and gamma density at around 2 - 2,5 m interval indicate terrestrial input. Below 3 m of the core section until 5 m gamma density properties show uniform distribution indicating no sudden change in lithology. However, magnetic susceptibility values at same interval increase abruptly, indicating iron-rich mineral accumulation. Magnetic susceptibility values continue to increase slightly from 5 m up to 7.8 m of the core section. Fluctuating gamma density values for this interval is due to material changes and the abundance of shells and shell fragments in the sediment. Between 7,8 m and 8,4 m magnetic susceptibility values show distinct decrease, indicating increasing amount of shell rich material. Distinct decrease in gamma density values corresponds abrupt increases of fractional porosity values at around 8 m shows the changes in material at this level. Increasing magnetic susceptibility values below the boundary shows the increasing grain size. Following this abrupt increase between 8,4 m and 9,5 m of core interval continues to increase slightly uniform until the bottom of the core. Gamma density distribution along the interval shows slightly uniform trend with negative correlation of certain levels corresponding positive correlation of fractional porosity.

### **3.3 XRF RESULTS**

In this section element profile results, using the ITRAX XRF-Core Scanner are given for following elements; Si, K Ca, Ti, Cr, Mn, Fe, Ni, Zn, Rb, Sr, Zr, Pb. These elements are plotted because they are the ones that give important values for this core section.

- **Silicon**

Silicon element is known as an important terrigenous or productivity indicator. Si may provide a proxy for the origin of the sediment. Higher values reflect typically cold - wet periods.

The XRF elemental profile for Si is presented in Fig. 21 Column 1. Uppermost 9 m of the core interval fluctuates similar to K element, except minor changes. Si shows

higher values at around 10 m to 11 m of the core. Below this interval Si record shows a sudden decrease in concentration and slightly increases until the bottom of the core.

- **Calcium**

Calcium element is an obvious indicator for carbonate minerals and its negative correlation with trace element confirms the important role of clay minerals, while positive correlation of Ca values is principally associated with sand grains and shell content.

The XRF elemental concentration for Ca is plotted in Fig. 21 column 3. The abundance peaks of the Ca occur during the historical warm periods. The uppermost 1 m of the Calcium values fluctuate from the top to the bottom of the core interval. At around 0.5 m slightly increase but slightly decrease downcore. From 1 m up to 2 m Ca shows a uniform distribution along the core interval. Below this level Ca profile shows abrupt changes until 4 m core depth. The highest amounts of Ca values throughout this interval are observed between 2 - 2,3 m, 2,9 - 3,1 m and 3,4 - 4 m. Calcium profile shows positive excursions between 4 m and 8 m interval, where shells and shell fragments are present also observed from the radiographic image. Below this level until the end of core, Ca profile has practically uniform distribution with slight changes, except for minor decrease in 9 m of the core section.

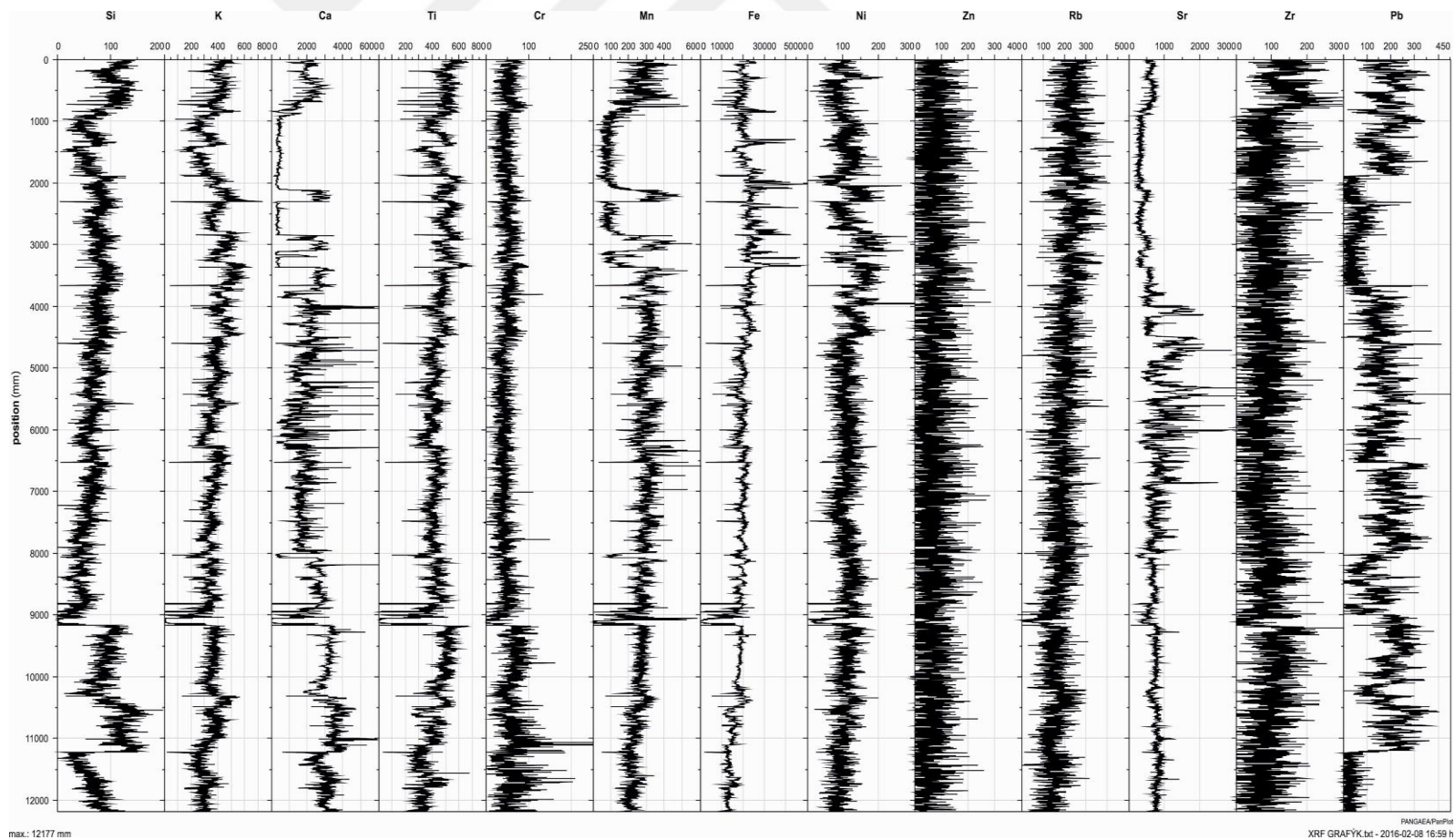


Figure 21. XRF/depth profiles of Si, K Ca, Ti, Cr, Mn, Fe, Ni, Zn, Rb, Sr, Zr, Pb.



- **Potassium and Titanium**

The potassium concentrations are primarily a function of clay mineral content. This element enters into the system with detrital clay minerals. High K values may indicate porosity increasing. Titanium indicates that there is terrigenous input in the environment. These elements show very similar patterns and close correlations along the core.

The XRF elemental profiles for K and Ti are demonstrated in Fig 21 column 2 and 4. K and Ti profiles shows uniform distribution along the core section with negative excursions corresponding to positive excursions of Calcium profile. Fe, K and Ti profiles demonstrate similar distribution along the core, except minor increase in 1,5 – 3,5 m interval where Fe profile shows positive excursions. Fe peaks are also in correlation with where iron dots are observed and added to the visual core description.

- **Iron**

The XRF elemental profile for Fe is presented in Fig. 21 column 7. Iron distributions are also primarily associated with clay minerals and shows similar patterns and close correlations as K and Ti along the core, except 1,5 m to 3,5 m interval shows positive excursions. Iron values decrease slightly until the end of the core. Ca enrichment is observed where Fe decreases. Higher values Fe commonly seen in oxic parts of the sediment.

- **Manganese**

Rock - forming ferromagnesian minerals contain considerable amount of Manganese. Much of the Mn accumulation along the core is in correlation with the detrital material carried by Kızılırmak River. The XRF elemental profile for Mn is presented in Fig. 21 column 6. Manganese profiles show high values in the uppermost 1 m of the core. Starting from 1m up to 2 m core depth Mn values decreases distinctly, which is unassociated with Fe values. Decreasing Mn values correlates with organic rich material at same interval. Below this depth Mn shows high peak and decreasing values below this peak. At around 3 m of the core there is another peak and slight decrease below the peak. Mn profile demonstrates high values associated with Manganese profile shows slightly uniform downcore distribution with intermediate values below 4 m of the core. Below the boundary, Mn values decreases slightly, showing small up and down excursions until the bottom of the core.



- **Strontium**

Strontium element gives information about the paleoenvironment. Highest values of Sr may indicate shallow water source. Strontium and Calcium are one of the key parameters in estimation of paleoclimate and paleoenvironment. The clearest climatic data in XRF elemental analysis is derives from the Ca/Sr proportion. The XRF elemental profile for Sr is presented in Fig. 21 column 11. Sr values are low in the first 4 m of the core interval, and shows uniform distributions with minor changes. Below the 4 m boundary there is an abrupt change in Sr profile until the 7 m core. The maximum enrichment of Sr is observed within this interval and along the core at around 5.2 m – 6 m. After this interval Sr profile starts to decrease. Below 7 m boundary until the end of the core Sr values shows slightly uniform downcore distribution with low values and minor decreases.

- **Rubidium**

Rubidium element is primarily related with detrital clay minerals and may be enhanced in mud levels along the core. The XRF elemental profile for Rb is presented in Fig. 21 column 10. Rb profile does not show any significant changes along the core, except minor changes. They may show grain size related fluctuations. From top to bottom of the core, Rb element concentration decreases slightly, corresponding decreasing clay minerals and increasing sand size material throughout the core.

- **Zirconium**

Zirconium element concentrations are generally related to the areal distribution of clay minerals. The XRF elemental profile for Zr is presented in Fig. 21 column 9. Zr profile demonstrates uniform distribution with high values along the core, except the enrichment at the uppermost 1 m of the core. Zr and Ti elements are useful as an indicator of sediment source.

### 3.4 AMS RESULTS

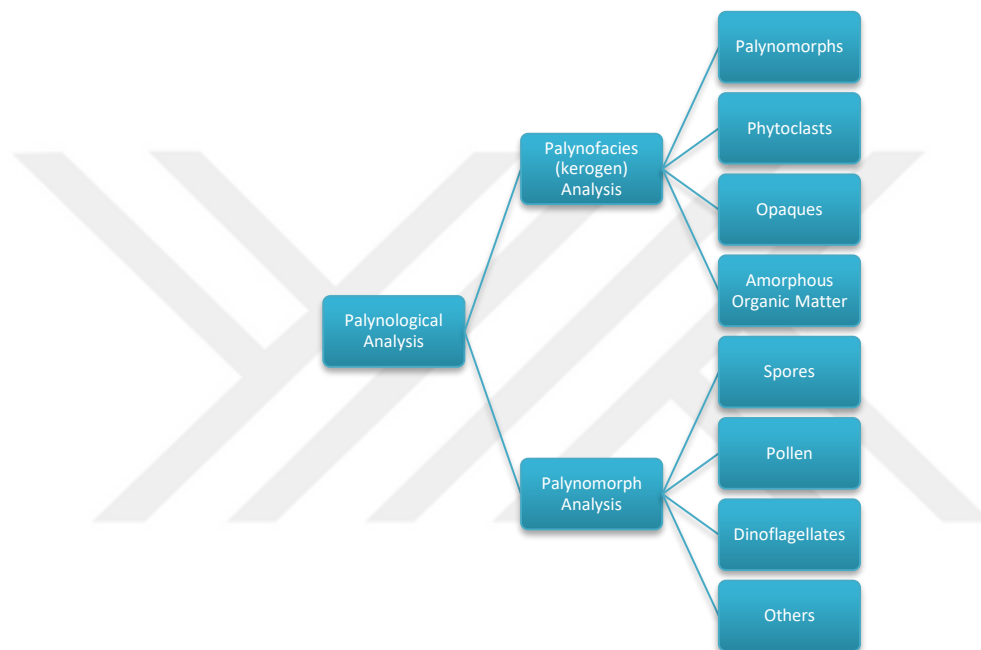
Ten accelerator mass spectrometry (AMS) radiocarbon ages were available for the whole sediment core. Only two ages are used for this study and they are presented in Table. 1.1.

**Table 1. AMS 14C dating results.**

Code	Core Depth (m)	Material	14c age a BP:	Calibrated age a. BP
RC-5	4,44-4,54	Cardium sp.	4090 +/- 30 BP	Cal BP 4305 to 3865
RC-0	13,25	Cardium sp.	7380 +/- 40 BP	Cal BP 7955 to 7645

### 3.5 PALYNOLOGICAL RESULTS

Palynological analysis basically have two types. Examination of slides prepared for Palynological analysis revealed using Palynofacies analysis make more sense, due to lack of pollen content. The term palynofacies was first introduced by Combaz in 1964. This method is used for characterisation of the depositional environment. Palynofacies analysis involves the identification of individual palynomorph, phytoclasts, opaques and amorphous organic matter.



Although we prepared 38 pollen samples for identification due to the time constraints of our partner in Comenius University, Slovakia we could not present the all results here. Here we present only four samples result. However, each pollen data correlates with one major lithostratigraphic unit out of four major unit. Therefore it is useful for correlation with the interpretations from other techniques.

Palynological analysis from 0-0,40 m interval revealed;

- Freshwater algae, *Spirogyra sp.*
- Plant tissue observed very well preserved, which indicates short transportation.
- Fungi

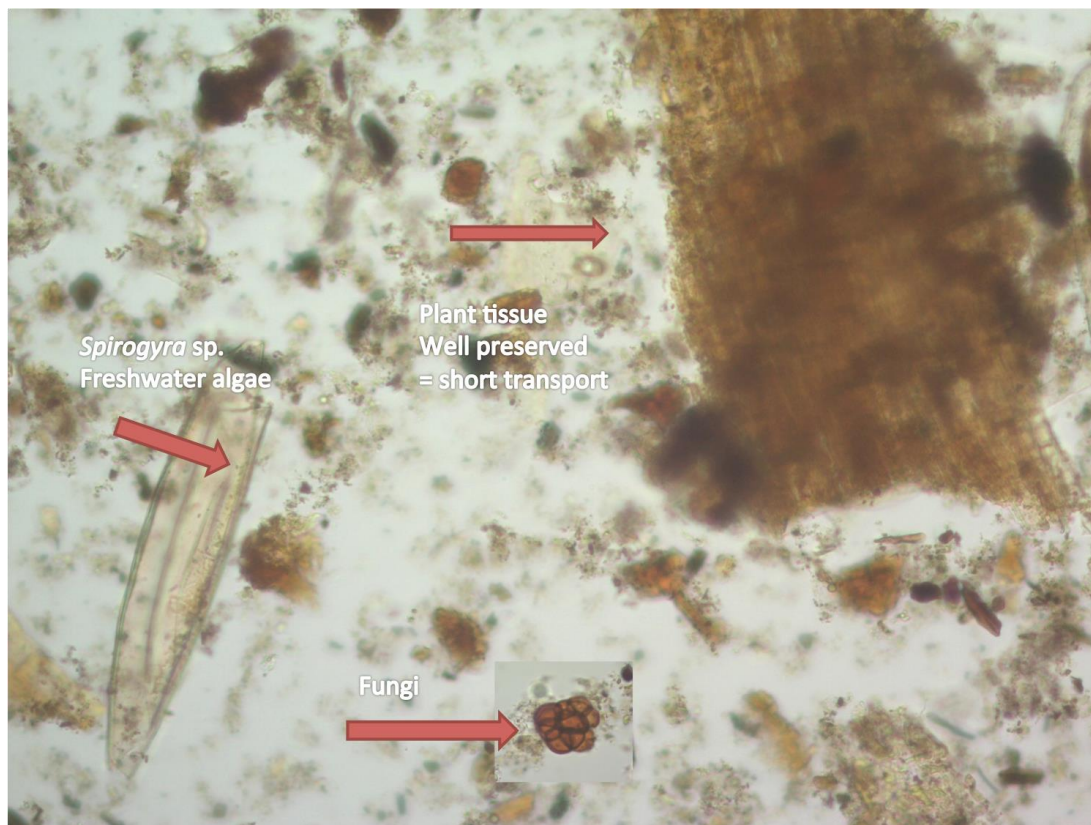


**Figure 22. Palynology results from 0-0,40 m interval**

Palynological analysis from 1,40-1,42 m interval revealed;

- Phytoclast
- Algae
- Fungi
- Freshwater algae, Botryococcus braunii
- Freshwater algae, Maugeotia

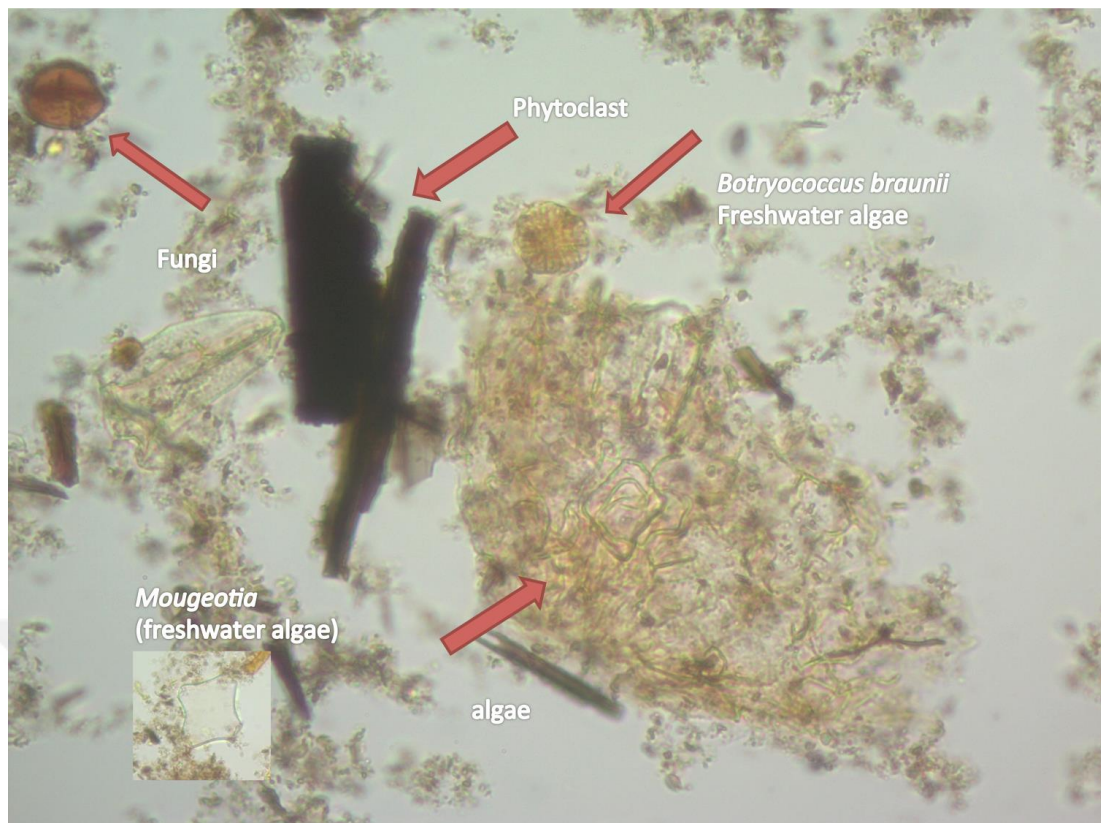


**Figure 23. Palynology results from 1,40-1,42 m interval**

Palynological analysis from 3,68-3,70 m interval revealed;

- %99 Amorphous organic matter, which indicates high potential for oil



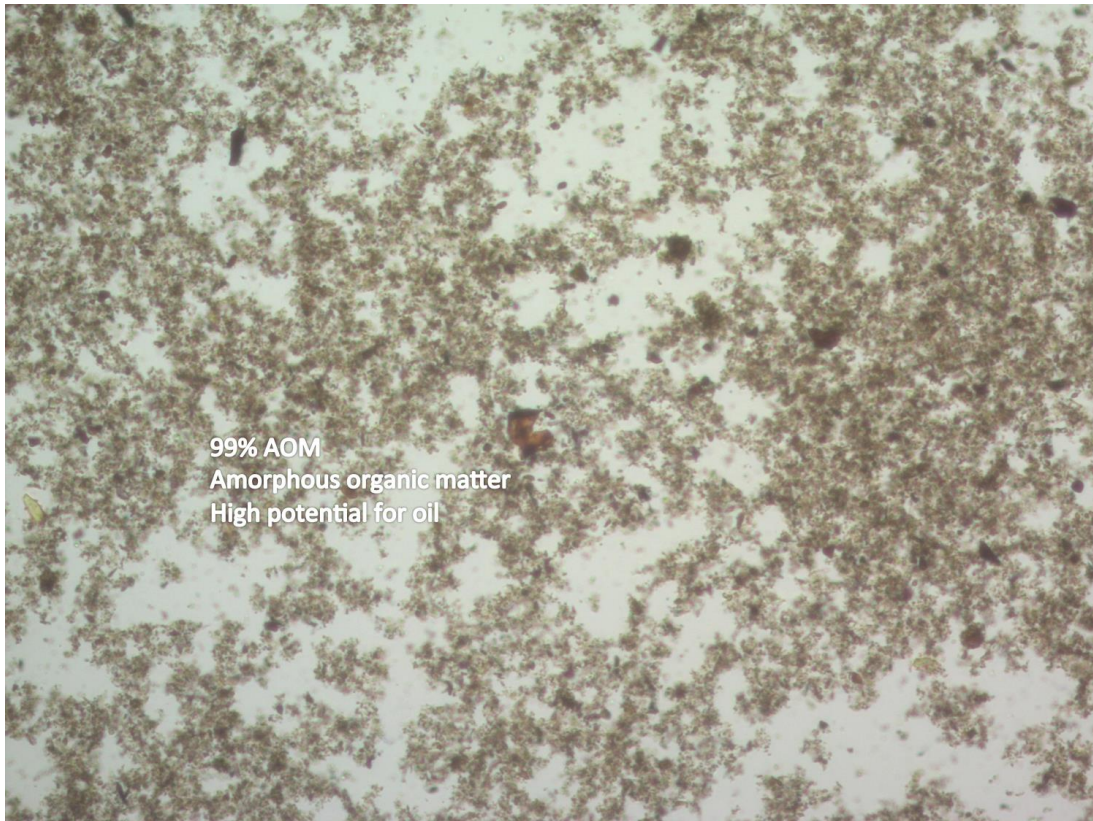


**Figure 24. Palynology results from 3,68-3,70 m interval**

Palynological analysis from 8,50-8,52 m interval revealed;

- %95 phytoclast content
- Freshwater algae
- Aquatic plants pollen



**Figure 25. Palynology results from 8,50-8,52 m interval**

The key to success of palynofacies work is combining the palynology with sedimentology and geochemistry. Results obtained from palynological analysis showed close correlation with the results of lithological interpretations and element profile results. This combination of analysis has led to read to development of the Kızılırmak Delta.

#### 4. DISCUSSION

In this chapter, results given in previous chapter are combined. The XRF analysis and lithological observations revealed the environmental development in four major unit. Lithological properties of sediment core, suggest an environment open marine, nearshore conditions in the first unit. This open marine conditions becomes restricted so that lagoonal conditions take place. The lagoon is well-oxygenated at the beginning but becomes restricted until only a lake environment with a high evaporation rate remains. On top sub-recent soil build-ups.

DEPTH	UNIT	GRAIN SIZE	INTERPRETATIONS	REMARKS
0 – 0.93 m	U4	Muddy fine sand	Soil	Flow structures, iron oxide dots, organic rich content
0.93 – 3.37 m	U3	Silty clay	Lake	Alternated Ca content High Fe/Mn High Sr/Ca
3.37 – 8.07 m	U2	Fine sandy mud	Lagoon	Lower Ca content Low Fe/Mn Medium-High Sr/Ca
8.07 – 12.18 m	U1	Fine to medium sand	Shallow Marine	High Ca content Low Fe/Mn Low Sr/Ca High fossil content



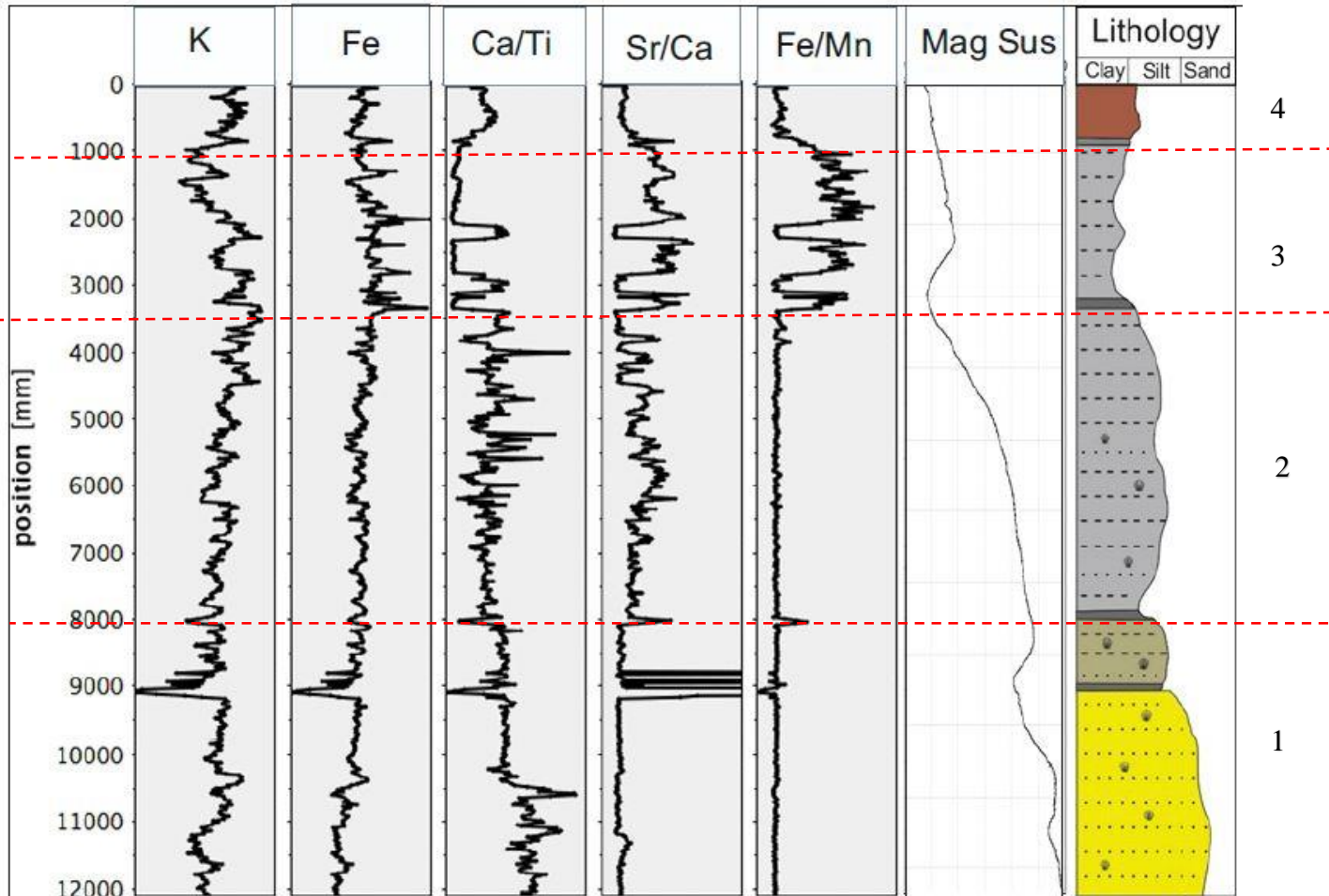


Figure 26. Lithological profile and certain elemental ratios of XRF ITRAX results of the sediment core BW-1

## 5. CONCLUSION

This study provides around 7300 year high-resolution sedimentological record of using a multi-proxy approach of a sediment core from the Kızılırmak Delta Plain in the Black Sea Region of Turkey. The post-glacial construction of the Kızılırmak Delta provides high sedimentation rates that gives the opportunity to analyze the development of the paleoenvironment. Four major lithostratigraphic units have been identified in the BW-1 core section, along with a number of sub-units. Major lithostratigraphic unit shows an open marine, near shore conditions in the first unit (8.07- 12.18). This shallow marine conditions become restricted more over the times so that lagoonal conditions took place (3.37 - 8.07). Third unit shows lake conditions (0.93 – 3.37). Uppermost unit demonstrates sub-recent soil build-ups (0 – 0.93).

Sediments consisting green gray mud with shells indicating prevailing oxic conditions and consisting of gray-dark gray to black mud with indicating prevailing suboxic to anoxic conditions. There are four black organic rich mud levels along the core indicating anoxic conditions. Some sandy layers with shell fragments are preserved in the core and seem to be associated with periods of increased extreme sea events. The results for these coarse-grained layers may indicate historical storm events in this area.

Despite the limitations of a single core our results obtained from several methodologies (sedimentology, geochemistry and palynology) provide insights in the paleoenvironmental conditions. However, further investigations, such as microfaunal analysis, are needed to better constrain the reconstruction of sea level transfer function.

## REFERENCES

**AKKAN, E.**, 1970. Bafra Burnu - Delice Kavşağı arasında Kızılırmak Vadisinin Jeomorfolojisi, A.Ü. DTCF Yay No: 191, Ankara

**AKSU, A. E.**, et al. Seismic stratigraphy of Late Quaternary deposits from the southwestern Black Sea shelf: evidence for non-catastrophic variations in sea-level during the last~ 10 000 yr. *Marine Geology*, 2002, 190, No. 1, pp. 61-94.

**ARDOS, M.**, 1996, Türkiye’de Kuaterner Jeomorfolojisi, Çantay Kitabevi Yay., İstanbul

**AVSAR, N.B.**, Jin, S., Kutoglu, H., and Gurbuz, G. (2016) Sea level change along the Black Sea coast from satellite altimetry, tide gauge and GPS observations, *Geodesy and Geodynamics*, 7(1): 50-55.

**BADERTSCHER, S.**, Fleitmann, D., Cheng, H., Edwards, R.L., Göktürk, O.M., Zumbühl, A., Leuenberger, M., Tüysüz, O., 2011. Pleistocene water intrusions from the Mediterranean and Caspian seas into the Black Sea. *Nat. Geosci.* 4:236–239.

**BAHR, Andre**, et al. Abrupt changes of temperature and water chemistry in the late Pleistocene and early Holocene Black Sea. *Geochemistry, Geophysics, Geosystems*, 2008, 9, No. 1.

**BALABANOV, Igor P.** Holocene sea-level changes of the Black Sea. In: *The Black Sea Flood Question: Changes in Coastline, Climate, and Human Settlement*. Springer, 2007, pp. 711-730.

**COMBAZ, A.** 1964. Les palynofacies. *Revue de Micropaleontologie*, 7, 205-218. [SEP]

**COUR, P.**, 1974. Nouvelles techniques de détection des flux et des retombées polliniques. Etude de la sédimentation des pollens déposés à la surface du sol. *Pollen & Spores*, 16 : 103-141.

**CROUDACE, I. W.**, Rindby, A., & Rothwell, R. G. (2006). ITRAX: Description and evaluation of a new multi-function X-ray core scanner. *Geological Society, London, Special Publications*, 267(1), 51-63.

**DSİ**, 1986, Bafra Projesi Planlama Revizyon Raporu DSİ 7. Bölge Md., Samsun.

**DEMİRBAĞ, Emin**, et al. The last sea level changes in the Black Sea: evidence from the seismic data. *Marine Geology*, 1999, 157, No. 3, pp. 249-265.

**GRICE, K.** (2015). *Principles and practice of analytical techniques in geosciences*. Cambridge: Royal Society of Chemistry, 9,274.

**IVANOVA**, Elena et al. The Holocene Black Sea reconnection to the Mediterranean Sea: New insights from the northeastern Caucasian shelf. *Palaeogeography, Palaeoclimatology, Palaeoecology*, 2015, 427, p. 41-61.

**KULELI**, T, Senkal, O, and Erdem, M, 2009, National assessment of sea level rise using topographic and census data for Turkish coastal zone, *Environmental Monitoring and Assessment*, 156: 425–434.

**MAJOR**, C., Goldstein, S., Ryan, W., Lericolais, G., Piotrowski, A.M., Hajdas, I., 2006. The co-evolution of Black Sea level and composition through the last deglaciation and its paleoclimatic significance. *Quat. Sci. Rev.* 25 (17–18):2031–2047.

**MAZULLO**, J., & Graham, A. G. (1988). *Handbook for shipboard sedimentologists*.

**MSCL-S**. (n.d.). Retrieved August 25, 2016, from <http://www.geotek.co.uk/products/mscl-s>

**PLASTINO W**, Kaihola L, Bartolomei P, Bella F. 2001. Cosmic background reduction in the radiocarbon measurements by liquid scintillation spectrometry at the underground laboratory of Gran Sasso. *Radiocarbon* 43(2A):157–61.

**RAO**, A. G. (2006). *Core wall: A methodology for collaborative visualization of geological cores*. University of Illinois at Chicago, 11,136.

**REED**, Joshua Allen, " The Paleontological Stratigraphic Interval Construction and Analysis Tool" (2007). Retrospective Theses and Dissertations. Paper 15105.

**ROTHWELL**, R. G., & Rack, F. R. (2006). New techniques in sediment core analysis: An introduction. *Geological Society, London, Special Publications*, 267(1), 1-29.

**RYAN**, William BF, et al. An abrupt drowning of the Black Sea shelf. *Marine Geology*, 1997, 138, No. 1, pp. 119-126.

**RYAN**, W.B.F., Vachtman, D., McHugh, C., Çagatay, M.N., Mart, Y., 2013. A channeled shelf fan initiated by flooding of the Black Sea. In: Gofredo, S., Dubinsky, Z. (Eds.), *The Mediterranean Sea: Its History and Present Challenges*, pp. 11–27.

**RYAN**, William BF, et al. A channeled shelf fan initiated by flooding of the Black Sea. In: *The Mediterranean Sea*. Springer, Netherlands, 2014. pp. 11-27.

**SCHNURRENBERGER**, D.S., J.M. Russell, and K.R. Kelts, 2003. Classification of lacustrine sediments based on sedimentary components. *J. Paleolimnology* 29: 141-154.

**SCHRADER**, H.J., 1979. Quaternary paleoclimatology of the Black Sea basin. *Sediment. Geol.* 23 (1 4), 165–180.

**SHUMILOVSKIKH**, Lyudmila S; Arz, Helge W; Wegwerth, Antje; Fleitmann, Dominik; Marret, Fabienne; Nowaczyk, Norbert R; Tarasov, Pavel E; Behling, Hermann (2013): Vegetation and environmental changes in Northern Anatolia between 134 and 119ka recorded in Black Sea sediments. *Quaternary Research*, 80(3), 349-360

**SOULET**, G., Ménot, G., Garreta, V., Rostek, F., Zaragosi, S., Lericolais, G., Bard, E., 2011a. BlackSea“Lake”reservoir age evolution since the Last Glacial hydrologic and climatic implications.

**STOCKMARR**, J. (1971) Tablets with Spores Used in Absolute Pollen Analysis. *Pollen et Spores*, 13, 615-621.

**OZESMI**, U. (1999) Conservation Strategies for Sustainable Resource use in the Kızılırmak Delta, Turkey. University of Minnesota, Ph.D. Dissertation

**OZESMI**, U. (1999). Ecosystems in the Mind: Fuzzy Cognitive Maps of the Kızılırmak Delta Wetlands in Turkey.

**YANKO-HOMBACH**, Valentina, et al. Holocene marine transgression in the Black Sea: new evidence from the northwestern Black Sea shelf. *Quaternary International*, 2014, 345, pp. 100-118.

**WEGWERTH**, A et al. (2014): Meltwater events and the Mediterranean reconnection at the Saalian-Eemian transition in the Black Sea. *Earth and Planetary Science Letters*, 404, 124-135

## CURRICULUM VITAE

PHOTO

**Name Surname:** Gülgün ERTUNÇ

**E-Mail:** gulgunertunc@gmail.com

### Personal Details:

**Nationality** :Turkish

**Place of birth** :Ankara

**Date of birth** :03.03.1988

### Education:

MSc : Istanbul Technical University,  
Eurasia Institute of Earth Sciences, 2015-2017, Geodynamics

BSc : Hacettepe University,  
Department of Geological Engineering, 2007-2013  
Geological Engineering

High School : Çankaya Anadolu Lisesi, 2003-2006

### Foreign Languages:

English/Advanced

German/Intermediate

### Research Interests:

Sedimentology

Quaternary Geology

Paleoclimatology

Oceanography

### Computer & Lab Skills:

Microsoft Office programs

CorelDraw, PSICAT, AutoCAD, GRASS GIS

**Trainings and Seminars:**

Dokuz Eylul University, Institute of Marine Sciences and Technology Research Vessel "R/V K.Piri Reis

Faculty of Natural Sciences Department of Geology and Paleontology, Comenius University in Bratislava

**Projects:**

- TÜBİTAK Project No: 113Y436, "Knidos Fayı'nın deprem tekrarlama aralığının ve kayma hızının klor-36 yüzey yaşlandırma yöntemi ile belirlenmesi"
- TÜBİTAK Project No: 112Y087, "Ecemiş Fayı'nın Kuvaterner'deki Atım Hızının Kozmojenik Klor-36 Yüzey Yaşlandırma Yöntemiyle Belirlenmesi"

**PUBLICATIONS, PRESENTATIONS AND PATENTS ON THE THESIS:**

Berndt, C., Ertunç, G., Yıldırım, C., Çiner, A., Sarıkaya, M.A., Öztürk, T., Güneç Kıyak, N. 2016. Timing and development of Late Quaternary fluvial terraces of the lower course of Kızılırmak River (Northern Turkey). European Geosciences Union General Assembly 2017, Vienna, Austria.

Berndt, C., Ertunç, G., Yıldırım, C., Çiner, A., Sarıkaya, M.A., Öztürk, T., Güneç Kıyak, N. 2016. OSL dating of fluvial strath terraces and paleo-delta levels of the Kızılırmak River: Implications for the uplift of the central Pontides. AGU Fall Meeting, 12-16 December, San Francisco, USA.

Berndt, C., Ertunç, G., Yıldırım, C., Çiner, A., Sarıkaya, M.A., Öztürk, T., Güneç Kıyak, N. 2016. OSL dating of fluvial strath terraces and paleo-delta levels of the Kızılırmak River: Implications for the uplift of the central Pontides. VII. Quaternary Symposium of Turkey (TURQUA), 8-11 May, Istanbul, Turkey, 24.

Berndt, C., Ertunç, G., Çiner, A., Yıldırım, C., Sarıkaya, M.A. 2016. Post-glacial development of the Black Sea level during Kızılırmak Delta build-up: Insights from microfaunal analysis. 69<sup>th</sup> Geological Congress of Turkey, 11-15 April, Ankara, Turkey, 598.

Berndt, C., Ertunç, G., Yıldırım, C., Çiner, A., Sarıkaya, M.A., Öztürk, T., Güneç Kıyak, N. 2016. OSL dating of fluvial strath terraces and paleo-delta levels of the Kızılırmak River: Implications for the uplift of the central Pontides. 69<sup>th</sup> Geological Congress of Turkey, 11-15 April, Ankara, Turkey, 477

**Extracurricular Activities:****Domestic:**

Project Coordinator, Youth Exchange Action 1.1: How Are We Affected By Euro Crisis? Let's Speaking About Solutions in Turkey (2013)

Participant, Practical Entrepreneurship Training, Ankara (2013)

**International:**

Participant, Youth Exchange Action 1.1: Prejuicios Fronterizos in Spain (2013)

Participant, Youth Exchange Action 3.1 : Art of Peace in Greece (2013)

Participant, Youth Exchange Action 4.3: Being a Volunteer Seminar in Greece (2013)

Participant, International Volunteer Youth Project in France (2011)

Participant, International Volunteer Youth Project in Italy (2010)

Participant, International Volunteer Youth Project in Germany (2009)

Participant, International Volunteer Youth Project in Germany (2008)